

SANDIA REPORT

SAND2005-5598

Unlimited Release

Printed September 2005

High Pressure Sulfuric Acid Decomposition Experiments for the Sulfur-Iodine Thermochemical Cycle

Fred Gelbard, James C. Andazola, Gerald E. Naranjo, Carlos E. Velasquez,
and Andrew R. Reay

Prepared by

Sandia National Laboratories

Albuquerque, New Mexico 87185 and Livermore, California 94550

Sandia is a multiprogram laboratory operated by Sandia Corporation,
a Lockheed Martin Company, for the United States Department of Energy's
National Nuclear Security Administration under Contract DE-AC04-94AL85000.

Approved for public release; further dissemination unlimited.



Sandia National Laboratories

Issued by Sandia National Laboratories, operated for the United States Department of Energy by Sandia Corporation.

NOTICE: This report was prepared as an account of work sponsored by an agency of the United States Government. Neither the United States Government, nor any agency thereof, nor any of their employees, nor any of their contractors, subcontractors, or their employees, make any warranty, express or implied, or assume any legal liability or responsibility for the accuracy, completeness, or usefulness of any information, apparatus, product, or process disclosed, or represent that its use would not infringe privately owned rights. Reference herein to any specific commercial product, process, or service by trade name, trademark, manufacturer, or otherwise, does not necessarily constitute or imply its endorsement, recommendation, or favoring by the United States Government, any agency thereof, or any of their contractors or subcontractors. The views and opinions expressed herein do not necessarily state or reflect those of the United States Government, any agency thereof, or any of their contractors.

Printed in the United States of America. This report has been reproduced directly from the best available copy.

Available to DOE and DOE contractors from

U.S. Department of Energy
Office of Scientific and Technical Information
P.O. Box 62
Oak Ridge, TN 37831

Telephone: (865)576-8401
Facsimile: (865)576-5728
E-Mail: reports@adonis.osti.gov
Online ordering: <http://www.osti.gov/bridge>

Available to the public from

U.S. Department of Commerce
National Technical Information Service
5285 Port Royal Rd
Springfield, VA 22161

Telephone: (800)553-6847
Facsimile: (703)605-6900
E-Mail: orders@ntis.fedworld.gov
Online order: <http://www.ntis.gov/help/ordermethods.asp?loc=7-4-0#online>



SAND2005-5598
Unlimited Release
September 2005

High Pressure Sulfuric Acid Decomposition Experiments for the Sulfur-Iodine Thermochemical Cycle

Fred Gelbard, James C. Andazola, Gerald E. Naranjo,
Carlos E. Velasquez, and Andrew R. Reay

Advanced Nuclear Concepts Department
Sandia National Laboratories
PO Box 5800
Albuquerque, NM 87185

ABSTRACT

A series of three pressurized sulfuric acid decomposition tests were performed to (1) obtain data on the fraction of sulfuric acid catalytically converted to sulfur dioxide, oxygen, and water as a function of temperature and pressure, (2) demonstrate real-time measurements of acid conversion for use as process control, (3) obtain multiple measurements of conversion as a function of temperature within a single experiment, and (4) assess rapid quenching to minimize corrosion of metallic components by undecomposed acid. All four of these objectives were successfully accomplished. This report documents the completion of the NHI milestone on high pressure H_2SO_4 decomposition tests for the Sulfur-Iodine (SI) thermochemical cycle project.

All heated sections of the apparatus, (i.e. the boiler, decomposer, and condenser) were fabricated from Hastelloy C276. A ceramic acid injection tube and a ceramic-sheathed thermocouple were used to minimize corrosion of hot liquid acid on the boiler surfaces. Negligible fracturing of the platinum on zirconia catalyst was observed in the high temperature decomposer. Temperature measurements at the exit of the decomposer and at the entry of the condenser indicated that the hot acid vapors were rapidly quenched from about 400 °C to less than 20 °C within a 14 cm length of the flow path. Real-time gas flow rate measurements of the decomposition products provided a direct measurement of acid conversion. Pressure in the apparatus was preset by a pressure-relief valve that worked well at controlling the system pressure. However, these valves sometimes underwent abrupt transitions that resulted in rapidly varying gas flow rates with concomitant variations in the acid conversion fraction.

The first acid test was used to shakeout equipment and procedure problems before proceeding with tests at the higher pressures that are planned for the SI cycle. This test was performed on 7 July 2005 at an absolute pressure of 2 bars for a one hour acid injection period. From the temperature data, we may conclude that liquid acid vaporized before contacting the boiler walls that were maintained above 600 °C. The decomposer temperature varied between 750 °C and 950 °C during the test, but an incorrect setting on the heater controller caused the decomposer temperature to cycle about 30 °C every 8 minutes. This problem was not fully recognized during the test, but from a post-test review, the problem was obvious and easily corrected. Because of the significant variation in decomposer temperature, steady state conditions were probably not obtained in this experiment and there is significant scatter in the acid conversion fraction. The system pressure was not recorded for this test, but this problem was resolved for the subsequent tests.

The second acid test was performed on 18 July 2005 at a pressure of 6 bars for an hour and thirty six minute acid injection period. The oscillating heating of the decomposer was eliminated and more reliable conversion data were obtained. The decomposer temperature varied between 775 °C and 875 °C. The acid conversion fraction at this pressure increased from about 0.4 to 0.45 as the temperature increased.

The third acid test was performed on 20 July 2005 at a pressure of 11 bars for a two hour acid injection period. The decomposer temperature was varied in four 30 minute 25 °C increments between 750 °C and 850 °C. The acid conversion fraction increased from about 0.3 to 0.5 as the temperature increased. The conversion data at 6 and 11 bars are consistent with expected behavior of conversion fraction increasing as temperature increases. However, the measurements did not have the resolution needed to show the decrease in conversion fraction with increasing pressure. The data are bounded by the theoretical maximum conversion determined by thermodynamic equilibrium.

We are in the process of disassembling the apparatus for detailed inspection of the interior surfaces. The collected liquid effluent from all the tests is being analyzed to determine the corrosion product composition. Significant corrosion was observed, and post test examinations will be performed to identify the location and magnitude of corrosion. The location of the corrosion is important since the condensing section corrosion issues should be eliminated with the new apparatus design that replaces the condenser with a direct contact heat exchanger.

Table of Contents

ABSTRACT.....	3
Table of Figures.....	6
Table of Tables.....	9
I. Introduction.....	11
II. Description of Apparatus.....	12
II.1. Overview.....	12
II.2. Details of Apparatus Operation.....	12
III. Data Analysis.....	27
IV. Test Results.....	35
IV.1. Pressurized Acid Test #1.....	36
IV.2. Pressurized Acid Test #2.....	44
IV.3. Pressurized Acid Test #3.....	52
V. Conclusions.....	61
References.....	63

Table of Figures

Figure 1. Schematic of straight-through sulfuric acid boiler, catalytic decomposer, and rapid-quench condenser. Red shaded regions of the boiler and decomposer represent split-tube heaters. The color-coding for the thermocouple locations are: light green dots = locations inside the flow, and dark green dots = locations on the outside surface, and partial green shading = heater control thermocouples.....	13
Figure 2. Straight-through sulfuric acid boiler, catalytic decomposer, and rapid-quench condenser prior to installing heaters, insulation, and instrumentation.....	14
Figure 3. Fully instrumented straight-through sulfuric acid boiler, catalytic decomposer, and rapid-quench condenser.....	15
Figure 4. Ceramic tubes used for acid injection and sheathing a thermocouple from the top of the boiler flange. The green discoloration is due to deposition of corrosion products.....	17
Figure 5. Top of Hastelloy boiler showing the SiC packing and top of mullite tube. The SiC pellets were provided by Ceramatec (Salt Lake City, Utah).....	18
Figure 6. Two-inch diameter mullite tube with one closed-end.....	19
Figure 7. Split-tube heater for acid decomposer. This heater is similar to that used for the boiler. The power capacities of the boiler and acid decomposer split-tube heaters are 2200 W and 1650 W, respectively.....	22
Figure 8. Platinum catalyst on zirconia support. The catalyst on the right was used to process acid for three tests over a total of four and a half hours. This catalyst is light grey in color compared to the grey color of fresh catalyst on the left. The catalyst was purchased from CRI Catalyst Company, Houston, Texas.....	23
Figure 9. Slotted Hastelloy C276 plugs used to retain catalyst in the decomposer. The top four plugs are new, but the plug at the bottom of the picture was used for all the experiments in this report. Only one plug is required to support the catalyst for the vertical orientation of the decomposer used in the tests. The notch allows the plug to slide past thermocouple wells. The slots allow vapor to pass through the plug while retaining catalyst pellets.....	24
Figure 10. Vapor pressure of sulfur dioxide (Weast, 1988; Vargaftik, 1975).....	31
Figure 11. Gibbs free energy of reaction of SO ₃ to SO ₂ and ½ O ₂ per mole of SO ₃ reacted, (HSC 5.1 computer code, 2002).....	34
Figure 12. Boiler temperatures for pressurized acid test #1 at 2 bars performed on 7 July 2005. The curves labeled “Inside bed top”, “Center”, and “Outlet” correspond to thermocouples numbered 1, 4, and 5, respectively, in Table 1. The vertical broken lines on the left and right correspond to the times at which the acid pump was turned on and off, respectively.....	37
Figure 13. Decomposer temperatures for pressurized acid test #1 at 2 bars performed on 7 July 2005. The numbers in parentheses in the legend correspond to the thermocouple numbers in Table 1. The oscillation was due to an incorrect heater controller setting, which was corrected in subsequent tests. The vertical	

broken lines on the left and right correspond to the times at which the acid pump was turned on and off, respectively.....	38
Figure 14. Rapid quenching of fluid from decomposer to condenser for pressurized acid test #1 at 2 bars performed on 7 July 2005. The curves labeled “Bottom of decomposer” and “Top of condenser” correspond to thermocouples numbered 13 and 14, respectively in Table 1. The vertical broken lines on the left and right correspond to the times at which the acid pump was turned on and off, respectively.	40
Figure 15. Condenser temperatures for pressurized acid test #1 at 2 bars performed on 7 July 2005. The numbers in parentheses in the legend correspond to the thermocouple numbers in Table 1. The vertical broken lines on the left and right correspond to the times at which the acid pump was turned on and off, respectively.	41
Figure 16. Total gas flow rate of effluent for pressurized acid test #1 at 2 bars performed on 7 July 2005. The pressure was not recorded for this test. The vertical broken lines on the left and right correspond to the times at which the acid pump was turned on and off, respectively.....	42
Figure 17. Acid conversion fraction for pressurized acid test #1 at 2 bars performed on 7 July 2005. The temperature is that measured by thermocouple number 10, which was inserted into the catalyst bed. Experimental problems that caused the large scatter in this data set were corrected in subsequent tests.....	43
Figure 18. Boiler temperatures for pressurized acid test #2 at 6 bars performed on 18 July 2005. The curves labeled “Inside bed top”, “Center”, and “Outlet” correspond to thermocouples numbered 1, 4, and 5, respectively, in Table 1. The vertical broken lines on the left and right correspond to the times at which the acid pump was turned on and off, respectively.....	45
Figure 19. Decomposer temperatures for pressurized acid test #2 at 6 bars performed on 18 July 2005. The curves labeled “Above catalyst bed”, “Center”, and “Inside bed below control”, and “Below catalyst bed” correspond to thermocouples numbered 8, 9, 10, and 11, respectively in Table 1. The vertical broken lines on the left and right correspond to the times at which the acid pump was turned on and off, respectively.	46
Figure 20. Rapid quenching of fluid from decomposer to condenser for pressurized acid test #2 at 6 bars performed on 18 July 2005. The curves labeled “Bottom of decomposer” and “Top of condenser” correspond to thermocouples numbered 13 and 14, respectively in Table 1. The vertical broken lines on the left and right correspond to the times at which the acid pump was turned on and off, respectively.	47
Figure 21. Condenser temperatures for pressurized acid test #2 at 6 bars performed on 18 July 2005. The numbers in parentheses in the legend correspond to the thermocouple numbers in Table 1. The vertical broken lines on the left and right correspond to the times at which the acid pump was turned on and off, respectively.	48
Figure 22. Total gas flow rate of effluent and system pressure for pressurized acid test #2 at 6 bars performed on 18 July 2005. The vertical broken lines on the left and	

right correspond to the times at which the acid pump was turned on and off, respectively.	49
Figure 23. Acid conversion fraction for pressurized acid test #2 at 6 bars performed on 18 July 2005. The temperature is that measured by thermocouple number 10, which was inserted into the catalyst bed.	51
Figure 24. Boiler temperatures for pressurized acid test #3 at 11 bars performed on 20 July 2005. The curves labeled “Inside bed top”, “Center”, and “Outlet” correspond to thermocouples numbered 1, 4, and 5, respectively, in Table 1. The vertical broken lines on the left and right correspond to the times at which the acid pump was turned on and off, respectively.	53
Figure 25. Decomposer temperatures for pressurized acid test #2 at 11 bars performed on 20 July 2005. The curves labeled “Above catalyst bed”, “Center”, and “Inside bed below control”, and “Below catalyst bed” correspond to thermocouples numbered 8, 9, 10, and 11, respectively in Table 1. The vertical broken lines on the left and right correspond to the times at which the acid pump was turned on and off, respectively.	54
Figure 26. Rapid quenching of fluid from decomposer to condenser for pressurized acid test #3 at 11 bars performed on 20 July 2005. The curves labeled “Bottom of decomposer” and “Top of condenser” corresponds to thermocouples numbered 13 and 14, respectively in Table 1. The vertical broken lines on the left and right correspond to the times at which the acid pump was turned on and off, respectively.	55
Figure 27. Condenser temperatures for pressurized acid test #3 at 11 bars performed on 20 July 2005. The numbers in parentheses in the legend correspond to the thermocouple numbers in Table 1. The vertical broken lines on the left and right correspond to the times at which the acid pump was turned on and off, respectively.	56
Figure 28. Total gas flow rate of effluent and system pressure for pressurized acid test #3 at 11 bars performed on 20 July 2005. The vertical broken lines on the left and right correspond to the times at which the acid pump was turned on and off, respectively.	57
Figure 29. Acid conversion fraction for pressurized acid test #3 at 11 bars performed on 20 July 2005. The temperature is that measured by thermocouple number 10, which was inserted into the catalyst bed.	58
Figure 30. Comparison between conversion fractions at 6 and 11 bars over the temperature range 750 °C to 875 °C. The theoretical equilibrium limit of conversion is computed from Eq. (12).	59

Table of Tables

Table 1. Thermocouple placement.....	20
Table 2. Laboratory-scale sulfuric acid processor characteristics.	26
Table 3. Pressurized acid test conditions.	29
Table 4. Figure index numbers for plots.....	35

I. Introduction

Hydrogen is a nonpolluting energy carrier that can be produced from water and nuclear energy, both of which are not dependent on politically unreliable nations as suppliers. Nuclear energy could be used to produce electricity, which could then be used to dissociate water to make hydrogen. However, this process is at best only 30% efficient in using nuclear heat. As an alternative, thermochemical cycles are a potentially more attractive approach for hydrogen production because the projected efficiencies are on the order of 50% with an advanced nuclear reactor. The DOE-NHI (Department of Energy - Nuclear Hydrogen Initiative) Research & Development Plan identified the Sulfur cycles as the most promising of these cycles for use with nuclear heating. For sulfur-based cycles, the catalytic decomposition of sulfuric acid is the reaction that directly utilizes nuclear heat and this reaction is the focus of this report.

Catalytic decomposition of sulfuric acid has been studied and demonstrated previously (Brecher, et al., 1977; Farbman, 1976; General Atomics, 1986; Norman et al., 1981; Parker, 1982). The primary objective of this work is to demonstrate and quantify pressurized acid decomposition with vessels made from industrial materials. The second objective is to demonstrate real-time measurements of acid conversion for use as process control. By developing real-time instrumentation to measure acid decomposition, the third objective can be achieved by applying such instrumentation to obtain multiple measurements of conversion as a function of temperature within a single experiment. Finally, the fourth objective is to assess rapid quenching to minimize corrosion of metallic components by undecomposed acid.

This report describes the experimental approach taken to achieve these objectives. Section II provides a description of the apparatus and details of the equipment, including interconnections, system assembly, approach, and the diagnostic instrumentation. In addition, the test sequence and operations are described. Section III describes the method used to process the data to obtain the acid conversion fraction. The analysis also includes a comparison of the data to the maximum theoretical conversion achievable. Section IV presents experimental results in a series of six plots for each test. These plots are of temperatures throughout the system, pressure, and gas flow rate which were recorded every 5 seconds. From these data, the acid conversion fraction is calculated and presented for each test and over a range of temperatures. Section V provides an assessment of the current results and plans for future work.

II. Description of Apparatus

II.1. Overview

The apparatus for boiling, decomposing, condensing, and collecting liquid effluent is arranged for straight-through downward processing of acid as shown schematically in Figure 1. The units for these four processes are shown as the boiler, decomposer, condenser, and collection flask, respectively. This arrangement eliminates bends or curves where acid could collect, corrode, and accumulate corrosion products. Produced gases, which are primarily sulfur dioxide and oxygen, are separated by gravity from the cooled liquid in the collection flask. These gases are filtered through a mesh filter to remove acid fumes that may be suspended in the gas stream. A relief valve, which is indicated in Figure 1 as a “pressure-setting valve”, sets the system pressure. The bypass valve is closed during an experiment, and opened to release pressure at the end of an experiment. The composition of the released gas is determined by gas chromatography prior to measuring the total gas flow rate and subsequent venting to the atmosphere. The basic components of the apparatus are shown in Figure 2 prior to installing the heaters, insulation, and instrumentation. A picture of the complete apparatus with this equipment installed is shown in Figure 3.

II.2. Details of Apparatus Operation

The apparatus is on a concrete test pad that is enclosed on three sides by several stacked 3-foot high and 2-foot thick concrete blocks, which can be seen in the background of Figures 2 and 3. The fourth side of the test pad is open to a fenced-off unoccupied field for which the nearest structure is many miles away. The temperature, pressure, gas composition, and gas flow rate data are recorded in the control room that is located behind the blocks which are shown schematically on the left side of Figure 1 as a thick vertical line. Part of the control room outer wall can be seen in the top part of Figure 3. Bottles of compressed nitrogen and helium needed for purging and for the gas chromatograph, respectively, are stored and operated from the control room. Similarly, the acid pump, gas bypass valve, and heaters are operated from the control room.

During active experimental operations, all personnel are behind the concrete blocks, preferably in the control room. When approaching or disassembling the apparatus after a test, hand held sulfur dioxide monitors are used, and areas in which the sulfur dioxide level is above 1 part per million are evacuated. (Sulfur dioxide has an 8-hour Time Weighted Average Threshold Limit Value, i.e. exposure limit, of 2 parts per million.) Acid is pumped directly from a bottle adjacent to the apparatus and thus no liquid chemicals are stored in the control room. The acid pump and all heaters automatically shut down and an alarm is sounded if the pressure exceeds a set point slightly above the desired operating pressure of the experiment. Electrical power to the pump and heaters is also controlled by a lock-out/tag-out procedure for which only the project manager (Fred Gelbard) has a key.

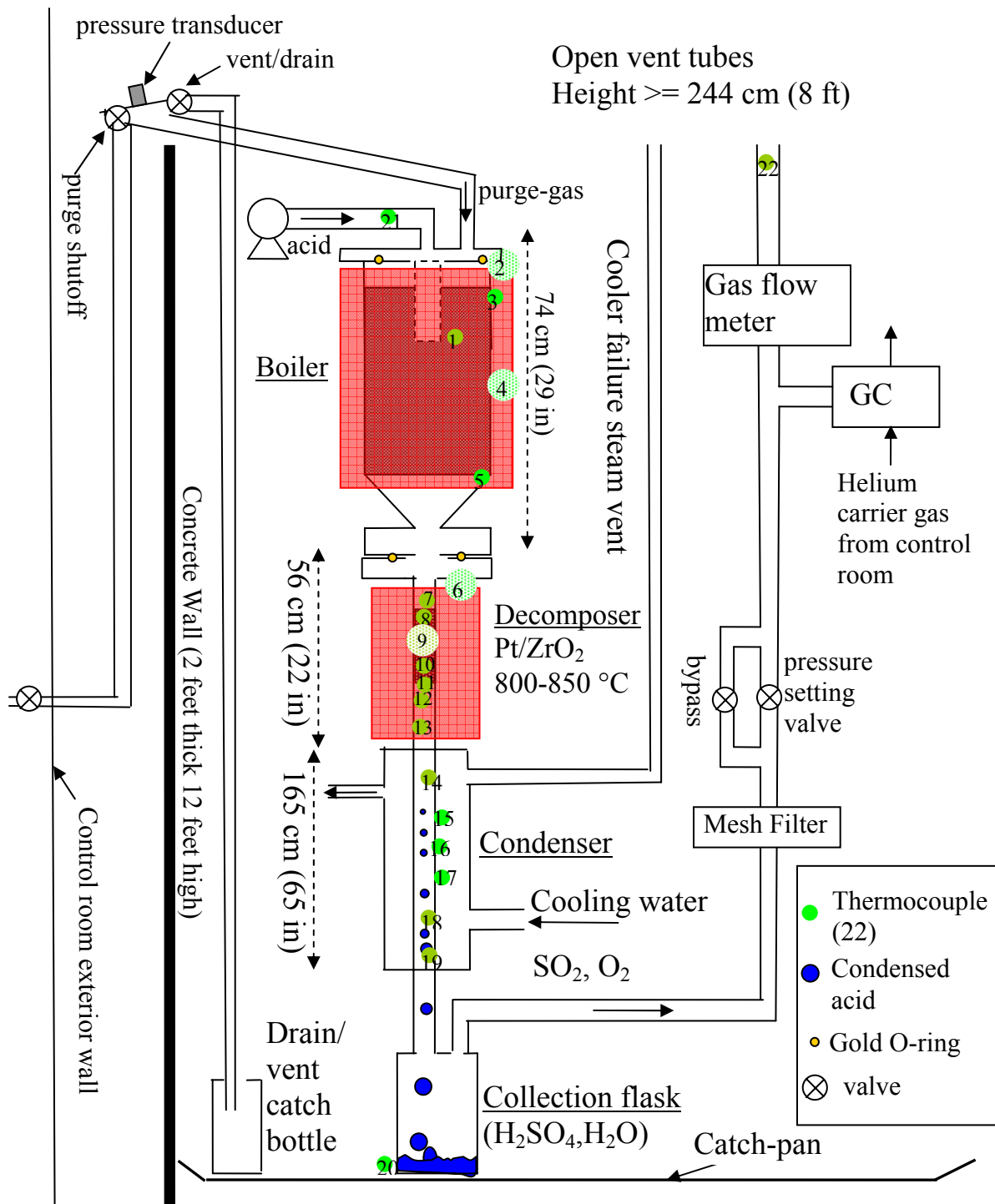


Figure 1. Schematic of straight-through sulfuric acid boiler, catalytic decomposer, and rapid-quench condenser. Red shaded regions of the boiler and decomposer represent split-tube heaters. The color-coding for the thermocouple locations are: light green dots = locations inside the flow, and dark green dots = locations on the outside surface, and partial green shading = heater control thermocouples.

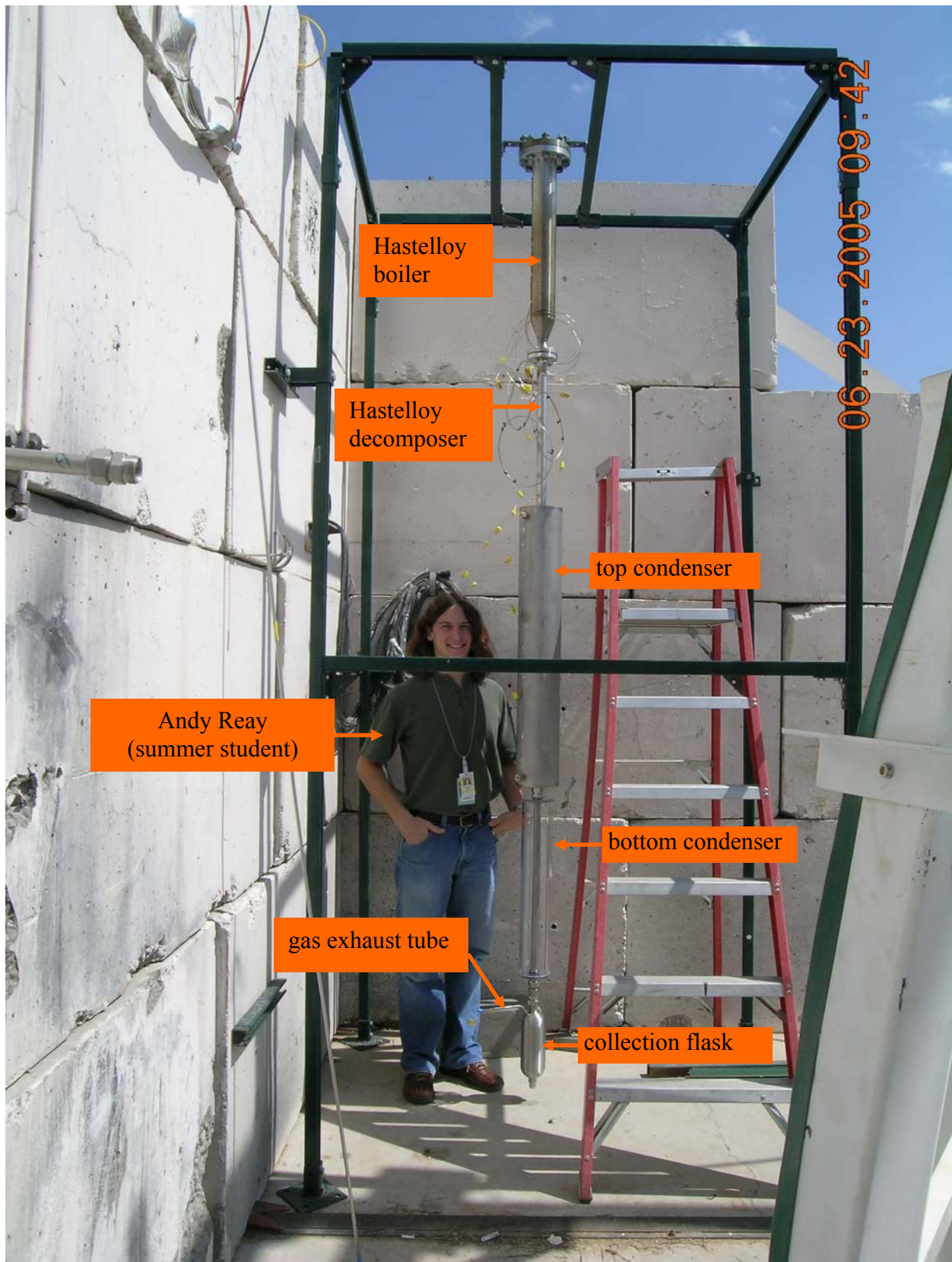


Figure 2. Straight-through sulfuric acid boiler, catalytic decomposer, and rapid-quench condenser prior to installing heaters, insulation, and instrumentation.

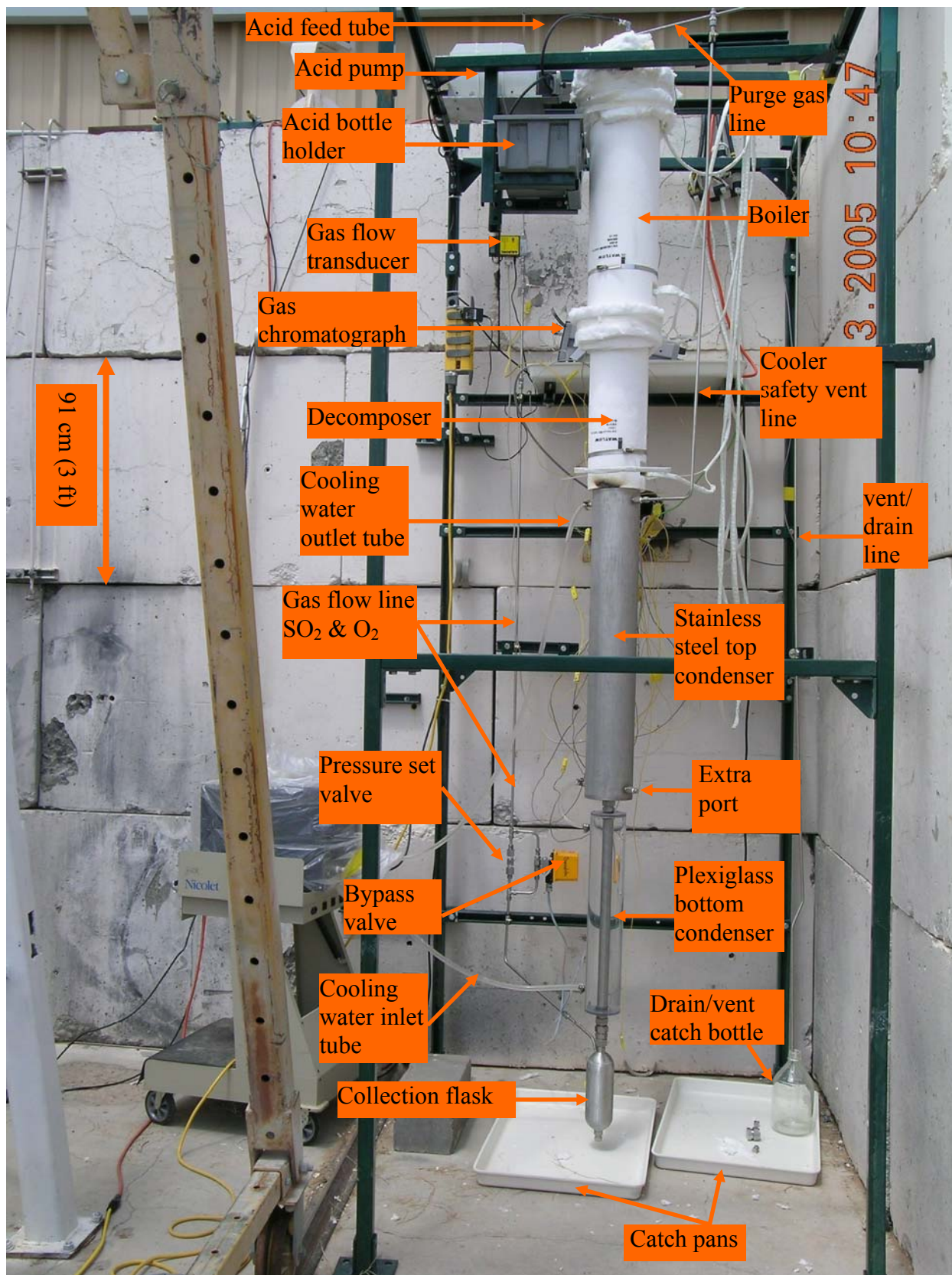


Figure 3. Fully instrumented straight-through sulfuric acid boiler, catalytic decomposer, and rapid-quench condenser.

Prior to starting an experiment, the pressure is set by installing a pressure-relief valve at the desired pressure. Then the purge shutoff and bypass valves are opened. Both these valves are

shown in the upper left corner of Figure 1, but only the pressure-relief valve, also called the pressure-setting valve, is shown in Figure 3. Then nitrogen is continuously released from a compressed gas bottle in the control room into the top of the boiler. Nitrogen is used to purge the apparatus of oxygen and sulfur dioxide that may have been retained from a previous test. This provides (1) a zero base oxygen concentration for the gas chromatograph, (2) a convenient test of the gas flow meter prior to acid injection, (3) assurance that there are no obstructions to flow, and (4) a means to test the operation of pressure-relief valve. The gas purge line can be seen at the top of Figures 1 and 3. The vent/drain valve shown in Figure 1 is generally closed, except if a clog develops which results in pressure buildup that cannot be released by opening the bypass valve. If such a problem occurs, gas and/or liquid can be safely vented and collected by operating this valve from behind the concrete barrier. In all the tests, this safety valve was not used because no clogs developed. After free flow of nitrogen has been confirmed, the split-tube heaters for the boiler and decomposer, the band heaters for the flanges, and the water chiller for the condenser are turned on. The heat up of the boiler and decomposer typically takes about three and a half hours.

Once the desired temperatures levels have been attained in the boiler and decomposer, the purge shutoff valve is turned off, and operations personnel are required to move to the control room for the remainder of the experiment. Acid processing begins with the remote starting of the acid pump, which injects pressurized acid through the top flange of the boiler. For acid pressures below 7 bars absolute (103 psia), a peristaltic pump is used. Above 7 bars a piston pump is used. The piston pump has the advantage that the flow rate can be controlled remotely from the control room in addition to being started and stopped remotely. Because the acid is at ambient temperature, viton, neoprene, or stainless steel tubing is used to pump unheated acid to the external top of the boiler without significant corrosion. Previously, Hastelloy tubing was used to inject acid from the boiler exterior through the top flange of the boiler. However, sulfuric acid is most corrosive when undergoing a phase change from liquid to gas, and this phase change occurred in the boiler near the acid injection tube. To avoid this corrosion problem, a ceramic injection tube made of alumina is used and is shown in top part of Figure 4. Similarly, instead of using a Hastelloy sheath for the top internal boiler thermocouple, a closed-end alumina tube is used as a thermocouple well and is shown in the bottom of Figure 4. This tube is also inserted through the top boiler flange.

The boiler is a 7.6 cm (3 in) diameter, 74 cm (29 in) long Hastelloy C276 pipe packed with 8 mm size silicon carbide (SiC) pellets that were provided by Ceramtec (Salt Lake City, Utah). Previously, 3.2-mm Denstone pellets were used, but the switch to silicon carbide was made because SiC has a much higher thermal conductivity. Therefore, fluid can be heated faster and more acid can be processed with the existing apparatus. To minimize the region in the boiler that requires heating, we adopted an idea used previously (General Atomics, 1986), and inserted concentrically into the boiler a hollow 5 cm (2 in) diameter mullite tube that is closed at one end. Thus, the acid flow is in the annular region between the mullite tube and the boiler wall. Approximately 2905 gm of SiC pellets are required to fill this annular region. A picture of the top of the boiler with SiC pellets is shown in Figure 5, and the mullite tube is shown in Figure 6. Additional SiC pellets are added to the boiler to cover the mullite tube shown in Figure 5.

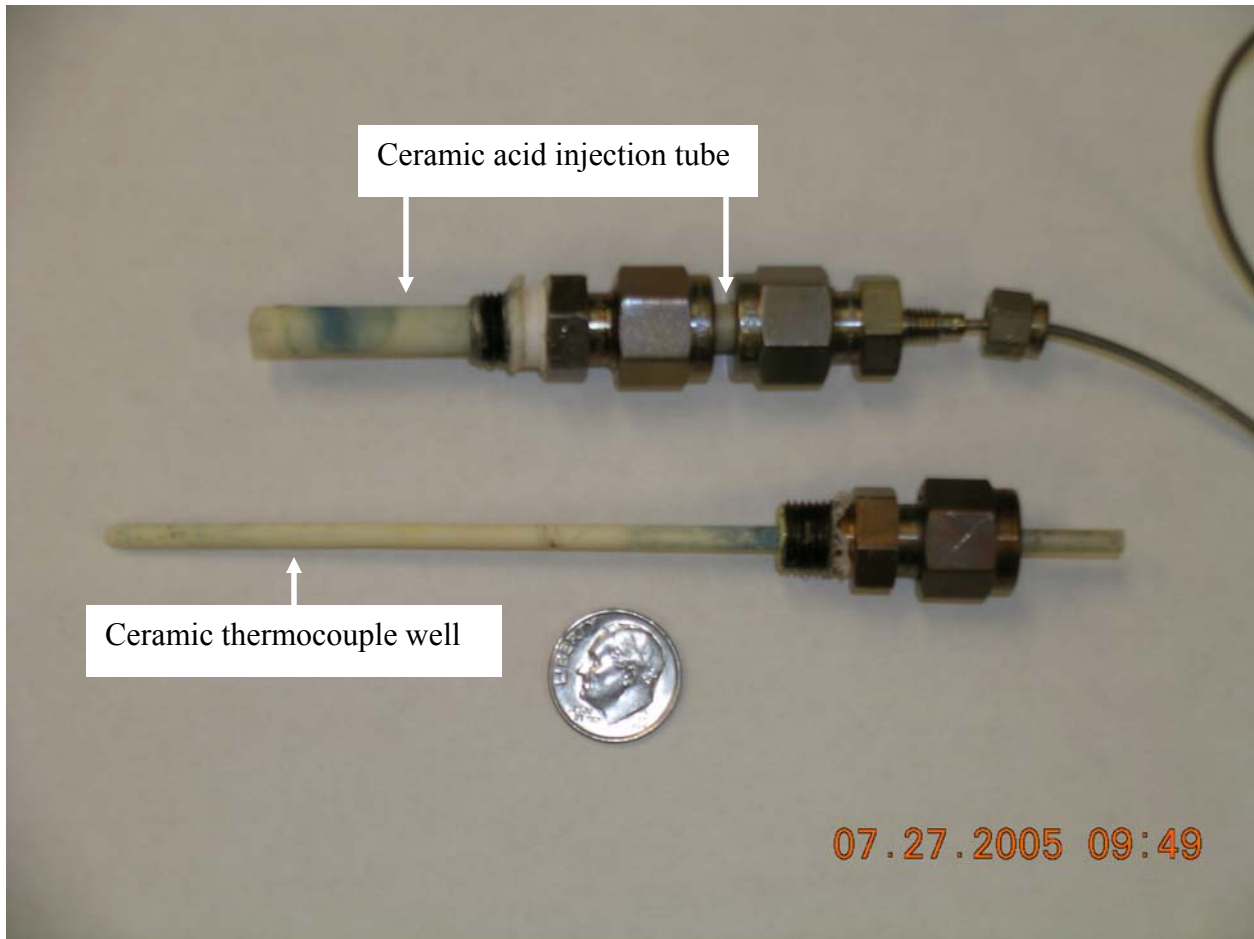


Figure 4. Ceramic tubes used for acid injection and sheathing a thermocouple from the top of the boiler flange. The green discoloration is due to deposition of corrosion products.

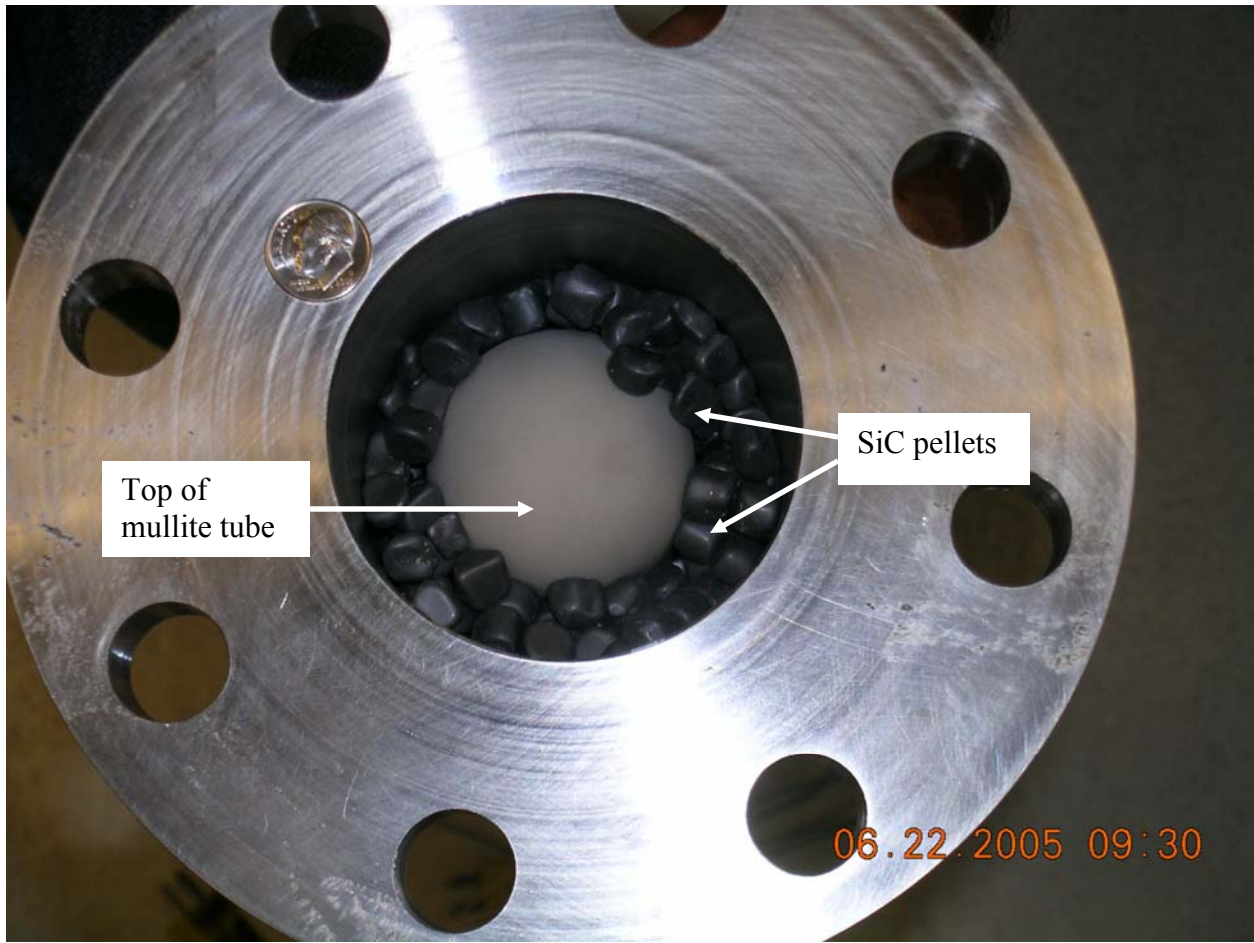


Figure 5. Top of Hastelloy boiler showing the SiC packing and top of mullite tube. The SiC pellets were provided by Ceramatec (Salt Lake City, Utah).



Figure 6. Two-inch diameter mullite tube with one closed-end.

The boiler is designed to have the liquid acid disperse as it falls through the SiC bed, and vaporize before reaching the boiler walls. The boiling point of sulfuric acid is 337 °C (Lide, 2001), and the boiler is designed to heat the fluid to ~500 °C, with the wall temperature well above 600 °C. Thus, all the acid solution is vaporized upon exiting the bottom part of the boiler and entering the decomposer. A split-tube heater encloses the boiler and provides up to 2200 W of power. In addition, a band heater surrounds the boiler top flange. Five thermocouples are used to monitor the boiler as shown schematically in Figure 1. Measurements from thermocouples numbered 2 and 4 are used as control variables for the band and split-tube heater controllers, respectively. All thermocouples are K-type and temperature readings are stored every 5 seconds. The locations of the thermocouples are given in Table 1.

Table 1. Thermocouple placement

Thermocouple Number	Thermocouple Location
1	Ceramic sheath inside top of boiler, ~ 2.5 cm (1 in) into top of SiC bed
2	Boiler top flange, control for band heater
3	Outside boiler wall, 1.5 inches (3.8 cm) from top flange
4	Outside boiler wall, 11 inches (28 cm) from top flange, control for split-tube heater
5	Outside boiler wall, 20 inches (51 cm) from top flange
6	Decomposer top flange, control for band heater
7	Inside decomposer, 3.5 inches (8.9 cm) below top flange and 1 inch (2.5 cm) above catalyst bed
8	Inside decomposer, 4.5 inches (11 cm) below top flange and flush with top of catalyst bed
9	Inside decomposer, 8.5 inches (22 cm) below top flange, inside catalyst bed, control for split-tube heater
10	Inside decomposer, 10.5 inches (26.7 cm) below top flange, inside catalyst bed
11	Inside decomposer, 12.5 inches (31.8 cm) below top flange, ½ inch below catalyst bed
12	Inside decomposer, 16.25 inches (41.3 cm) below top flange
13	Inside decomposer, 19.25 inches (48.9 cm) below top flange
14	Inside condenser, 24.75 inches (62.9 cm) below top flange
15	On outside condenser wall, 26.5 inches (67.3 cm) below top flange
16	On outside condenser wall, 28.75 inches (73 cm) below top flange
17	On outside condenser wall, 30.75 inches (78.1 cm) below top flange
18	Inside condenser, 44.75 inches (114 cm) below top flange
19	Inside condenser, 56.25 inches (143 cm) below top flange
20	Outside bottom of collection flask
21	Outside acid pump line (acid tests on 7 and 18 July 2005) Outside gas line just after collection flask (acid test on 20 July 2005)
22	On outside exhaust gas line

The bottom of the boiler is joined to a decomposer with a flange to allow for easy disassembly. The flanges are machined smooth and gold O-rings are compressed between the smoothed joints to create a tight corrosion-resistant seal. The decomposer consists of a Hastelloy C276 pipe 56 cm (22 in) long, with a 3.34 cm (1.315 in) outside diameter, and a wall thickness of 3.38 mm (0.133 in). A split-tube heater surrounds the decomposer and is shown in Figure 7.

From Table 1, thermocouples number 9 and 10 are inside the catalyst bed, with thermocouple number 8 flush with the top surface of the bed. To improve the measurements of the gas stream and catalyst bed temperatures, thermocouple wells that are 1.25 cm (0.5 in) long made from 3.18 mm (0.125 inch) Hastelloy tubing were welded radially inwards from the pipe walls, and thus extends ~9 mm into the flow. The thermocouple beads are secured at the bottom of these wells for thermocouples numbered 7 - 14, 18, and 19. These thermocouples are described in Table 1 as *inside* the region being measured, and are color-coded light green in Figure 1.

Approximately 134 grams of 1% Pt on zirconia catalyst is packed into the decomposer to form a packed bed that is 19 cm (7.5 in) long for all tests discussed in this report. The catalyst is in form of 4.8 mm diameter and length cylindrical pellets as shown in Figure 8, and is available from CRI Catalyst Company in Houston, Texas. The catalyst is supported by a slotted Hastelloy plug that is held in place by friction with the decomposer walls. This provides great flexibility in position the catalyst bed, and in this work the bottom plug was turned so that it also rested on top of thermocouple number 11 to fix the plug location. The slots provide a passage for vapor and a picture of these plugs is shown in Figure 9. One slot of the plug extends to the outer perimeter to form a notch such that the plug can slide past thermocouple wells that extend into the decomposer. In the center of the plug is a threaded hole such that a tool with a matching screw can be inserted into the hole to remove the plug.

Hot gas from the decomposer continues flowing down the Hastelloy pipe. The decomposer piping becomes a condenser that consists of two parts. The top part is a continuation of the Hastelloy pipe and is surrounded by a stainless steel water jacket. The bottom part is also a continuation of the pipe and is surrounded by a plexiglass water jacket. The lengths of the top and bottom condensers are 99 cm (39 in) and 63 cm (25 in), respectively, while the total condenser length including the space between the two cooling jackets is 165 cm (65 in). For convenience, in Figure 1 the condenser is shown as a single unit. Cooling water from the chiller is maintained at or below 10 °C and flows countercurrent to the vapor stream. If somehow the chiller pump fails, or the condenser wall fails and acid mixes with the cooling water, then the cooling water temperature would rise and start to boil. If this were to occur, steam would form in the water jackets and these jackets may not be able to hold the pressure. Therefore, a steam vent line that is open to the atmosphere is connected to the top of the stainless steel water jacket to serve as a relief in case of pressure buildup. This safety vent line is shown in Figures 1 and 3. The operating parameters of the boiler, decomposer, and condenser are summarized in Table 2.



Figure 7. Split-tube heater for acid decomposer. This heater is similar to that used for the boiler. The power capacities of the boiler and acid decomposer split-tube heaters are 2200 W and 1650 W, respectively.



Figure 8. Platinum catalyst on zirconia support. The catalyst on the right was used to process acid for three tests over a total of four and a half hours. This catalyst is light grey in color compared to the grey color of fresh catalyst on the left. The catalyst was purchased from CRI Catalyst Company, Houston, Texas.



Figure 9. Slotted Hastelloy C276 plugs used to retain catalyst in the decomposer. The top four plugs are new, but the plug at the bottom of the picture was used for all the experiments in this report. Only one plug is required to support the catalyst for the vertical orientation of the decomposer used in the tests. The notch allows the plug to slide past thermocouple wells. The slots allow vapor to pass through the plug while retaining catalyst pellets.

In previous experiments, most of the corrosion occurred in the condenser because hot liquid acid contacting the walls. To minimize this contact, Lloyd Brown (General Atomics, San Diego, California), suggested rapidly quenching the effluent from the decomposer. This approach was used previously and corrosion was not a reported problem (General Atomics, 1986). To evaluate rapid quenching, the condenser is a continuation of the same pipe used for the decomposer, and the water jacket for the condenser is placed as close as practical next to the bottom of the decomposer. This arrangement can be seen in Figure 3. To assess if the acid vapors are indeed rapidly quenched, a thermocouple is placed inside the flow with a thermocouple well at the bottom of the decomposer and another thermocouple at the top of the condenser. The distance between these thermocouples, numbers 13 and 14, respectively, can be readily determined from Table 1, and is 14 cm (5.5 in).

Undecomposed acid vapor and water produced by decomposition are collected in the stainless steel flask connected at the bottom of the condenser shown in Figures 1-3. The produced uncondensed gases, which are SO_2 and O_2 , are separated from the condensed liquid by gravity in the collection flask. These gases leave the flask through an exhaust tube and move up through a stainless steel mesh that is inside the vertical portion of the exhaust tube. The mesh is designed to capture acid fume and coalesce the fume droplets that may be entrained in the gas flow.

Gas that passes the mesh filter will continue to accumulate and thus increase the pressure throughout the apparatus until the pressure reaches the set pressure of the relief valve. Gas pressure is monitored from a pressure transducer that is located between the purge shutoff valve and the top of the boiler as shown in Figure 1. The bypass valve is closed during the experiment, and thus does not provide a path for gas release. This valve, however, is opened to relieve pressure after the experiment is completed. The gas released from the relief valve is analyzed for composition and flow rate. Previously, we attempted to use a fiber optic oxygen probe to determine the oxygen concentration of the released gas. However, that approach failed because the probe was deactivated by SO_2 , and therefore a gas chromatograph (GC) is now used in its place as shown in Figures 1 and 3. The GC has two columns and is capable of measuring vapor concentrations of O_2 , N_2 , H_2 , SO_2 , CO_2 , H_2S , and H_2O . A gas sample is analyzed every 3 minutes and the results are stored on a computer. The gas flow rate is monitored by a gas flow meter just prior to venting gas to the atmosphere. Data from the flow meter are stored every 5 seconds. The vent tube is 244 cm (8 ft) or more above ground level to ensure adequate dispersal of SO_2 .

At the end of an experiment, the heaters and acid pump are turned off and the bypass valve opened from within the control room to depressurize the apparatus. By using hand held gas monitors, the SO_2 level is measured outside the control room, behind the concrete barriers. The purge valve is opened if the SO_2 level is below 1 ppm. Then from within the control room, nitrogen is released through the purge line to remove residual SO_2 from the apparatus. Purging lasts overnight as the apparatus cools to ambient conditions prior to posttest analysis and preparation for the next test.

Table 2. Laboratory-scale sulfuric acid processor characteristics.

	Boiler	Catalytic Decomposer	Condenser
Operating Temperature	>500 °C (internal) >600 °C (wall)	750-950 °C	10 °C
Construction Material	Hastelloy C276	Hastelloy C276	Hastelloy C276
Dimensions	74 cm long, 7.5 cm diameter pipe	55 cm long, 2.5 cm diameter pipe	165 cm total length, 2.5 cm diameter
Fluid State	liquid/vapor	vapor	liquid
Packing	Silicon carbide 2905 gm and 2-in diameter hollow mullite tube	8 mm size pellets, 134 gm 1% Pt/ZrO ₂	none
Minimum Heating Required (100 l/hr SO₂)	330 W	337 W	none
Available Heating Capacity	2200 W	1650 W	none

III. Data Analysis

The key parameter to be determined from the experiment is defined as η , the fraction of acid converted to H_2O , SO_2 and O_2 as a function of pressure and temperature. In the experiments, these effluent gases, including undecomposed acid, are cooled to less than $20\text{ }^\circ\text{C}$, and the flow rates of **only** the uncondensed gases are measured. The gases that condense depend on the temperature and pressure in the condenser. To account for only uncondensed gases that are measured, we define β as the moles of uncondensed effluent gas per mole of decomposed acid. If only SO_2 and O_2 are uncondensed then $\beta = 1.5$ because for each mole of decomposed acid one mole of SO_2 and half a mole of O_2 are produced. However, if only O_2 is uncondensed then $\beta = 0.5$. As explained later, β varied between these values depending on the operating conditions of the experiment. With these definition for η and β , η is determined experimentally by,

$$\eta = \frac{1}{\beta} \left(\frac{f_{\text{gas}}}{f_{\text{acid}}} \right) \quad (1)$$

where

η = acid conversion fraction (dimensionless),

β = moles of uncondensed effluent gas/mole of decomposed acid (dimensionless),

f_{gas} = molar flow rate of uncondensed effluent gas (mol/min), and

f_{acid} = molar injection rate of acid (mol/min).

In the limit of no conversion, there are no measured gases produced in the experiment, thus $f_{\text{gas}} \rightarrow 0$ and $\eta \rightarrow 0$. In the other limit of complete acid conversion, $f_{\text{gas}}/f_{\text{acid}} \rightarrow \beta$ and therefore $\eta \rightarrow 1$.

This analysis neglects the removal from the gaseous effluent stream of SO_2 by dissolution in condensed acid. Measurements of pressurized SO_2 solubility in aqueous sulfuric acid have been reported at $25\text{ }^\circ\text{C}$ and $50\text{ }^\circ\text{C}$ at pressures up to 4 bars (Hayduk et al., 1988). The solubility is generally less than 0.1 SO_2 mole fraction, and is therefore a small correction. In addition, as noted in the paper, the “dissolution process required the use of the stirrer and that the amount of gas dissolved during the initial charging period was negligibly small.” In these dissolution experiments, the time to dissolve the gas with stirring required at least one hour. In the tests in this work there is no stirring of the solution. Thus SO_2 dissolution in condensed acid is neglected.

The uncondensed gas molar flow rate can be determined from the measured uncondensed gas volumetric flow rate and the ideal gas law, and is given by,

$$f_{\text{gas}} = \frac{PV}{RT} \quad (2)$$

where

\underline{V} = measured volumetric uncondensed gas flow rate (liters/min),

P = pressure at which uncondensed gas flow rate is measured (12.5 psia in Albuquerque, New Mexico),

R = ideal gas constant (1.206 liter-psia/mol-K),

T = gas temperature where the uncondensed gas flow rate is measured (typically 310 K for the tests), and

f_{gas} = uncondensed gas molar flow rate (mol/min).

Substituting Eq. (2) into Eq. (1) provides the expression needed to determine the acid conversion fraction from the data, and is given by,

$$\eta = \frac{1}{\beta} \left(\frac{PV}{RTf_{\text{acid}}} \right). \quad (3)$$

Note that the temperature and pressure in Eq. (3) are for the conditions at the flow meter, but the resulting value for η is for the temperature and pressure of the catalyst in the decomposer. This is based on the model that SO_3 decomposes to SO_2 and O_2 only in the catalyst-packed region of the decomposer, and the uncondensed gas molar flow rates measured at the flow meter are the same as those just past the catalyst. The pressure in the system is uniform between the purge shutoff valve and the pressure-setting valve. Therefore, the pressure measured by the pressure transducer is the same as that in the decomposer which is to be associated with the measured value of η . Pressure uniformity was verified by the observation that the preset value for the relief valve was in good agreement with the measured pressure attained in the system. The acid molar injection rate needed for Eq. (3) varied for the three tests as given in Table 3. Eq. (3) and the decomposer temperature data are used to construct plots of acid conversion fraction in this report.

Table 3. Pressurized acid test conditions.

	Test Number 1	Test Number 2	Test Number 3
Date of test	7 July 2005	18 July 2005	20 July 2005
Operating pressure	1.9 bars absolute (15 psig)	6.0 bars absolute (75 psig)	10.9 bars absolute (145 psig)
Acid injection rate	4 ml/min = 0.070 mol/min	4.2 ml/min = 0.074 mol/min	2.9 ml/min = 0.050 mol/min
Injected acid concentration	96.5 wt% = 83.5 mol% ($\gamma = 1.20$)	96.5 wt% = 83.5 mol% ($\gamma = 1.20$)	95.5 wt% = 79.6 mol% ($\gamma = 1.26$)
β	1.5	1.5	1.07
Duration for acid pumping	1 hour	1 hour 36 min	2 hours
Heater turn on time	12:53	~9:30	9:45
Acid pump start time	16:19	12:59 (shut down between 13:25-13:30)	13:13
Acid pump stop time	17:19	14:41	15:13

In the condenser and collection flask, the temperature is low and for pressures of 2 to 11 bars, nearly all the water vapor and unreacted acid can be expected to condense to an aqueous acid solution, and nearly all the produced oxygen will not condense. However, for an ideal gas mixture, SO₂ will condense if the partial pressure of SO₂ is greater than the equilibrium vapor pressure of pure SO₂. Let the equilibrium vapor pressure of pure SO₂ be given by $P_{\text{SO}_2, \text{eq}}$. An ideal gas mixture of one third oxygen and two thirds sulfur dioxide leaving the condenser will retain this molar concentration ratio up to a total pressure of $(3)(P_{\text{SO}_2, \text{eq}})/2$. Above $(3)(P_{\text{SO}_2, \text{eq}})/2$ total pressure, SO₂ will condense until the SO₂ partial pressure is reduced to $P_{\text{SO}_2, \text{eq}}$, with the remaining gas being O₂. If this equilibrium state is attained in the collection flask, then the ratio of the SO₂ partial pressure to the oxygen partial pressure is $P_{\text{SO}_2, \text{eq}} / (P - P_{\text{SO}_2, \text{eq}})$, where P is the total pressure in bars. Then the moles of uncondensed SO₂ for half a mole of O₂ is $(1/2)(P_{\text{SO}_2, \text{eq}} / (P - P_{\text{SO}_2, \text{eq}}))$. The total moles of uncondensed gas per mole of decomposed acid is therefore given by,

$$\beta = \begin{cases} 1.5 & P < \frac{3}{2} P_{\text{SO}_2, \text{eq}} \\ \frac{1}{2} \left[\frac{P}{P - P_{\text{SO}_2, \text{eq}}} \right] & P \geq \frac{3}{2} P_{\text{SO}_2, \text{eq}} \end{cases} \quad (4)$$

In the limit of high pressure ($P \gg P_{\text{SO}_2, \text{eq}}$), all the SO_2 is condensed and $\beta \rightarrow 0.5$.

The temperature of the fluid in the collection flask can be determined from thermocouple number 20 that was placed on the outside of the stainless steel collection flask. The temperature was about 38 °C throughout experiments at 6 and 11 bars. This was also the temperature measured on the exhaust tube from the collection flask with thermocouple number 21 for the test at 11 bars. From Figure 10, $P_{\text{SO}_2, \text{eq}} = 5.87$ bars at 38 °C. Thus from Eq. (4) $\beta = 1.5$ for the tests at 2 and 6 bars, and $\beta = 1.07$ for the test at 11 bars.

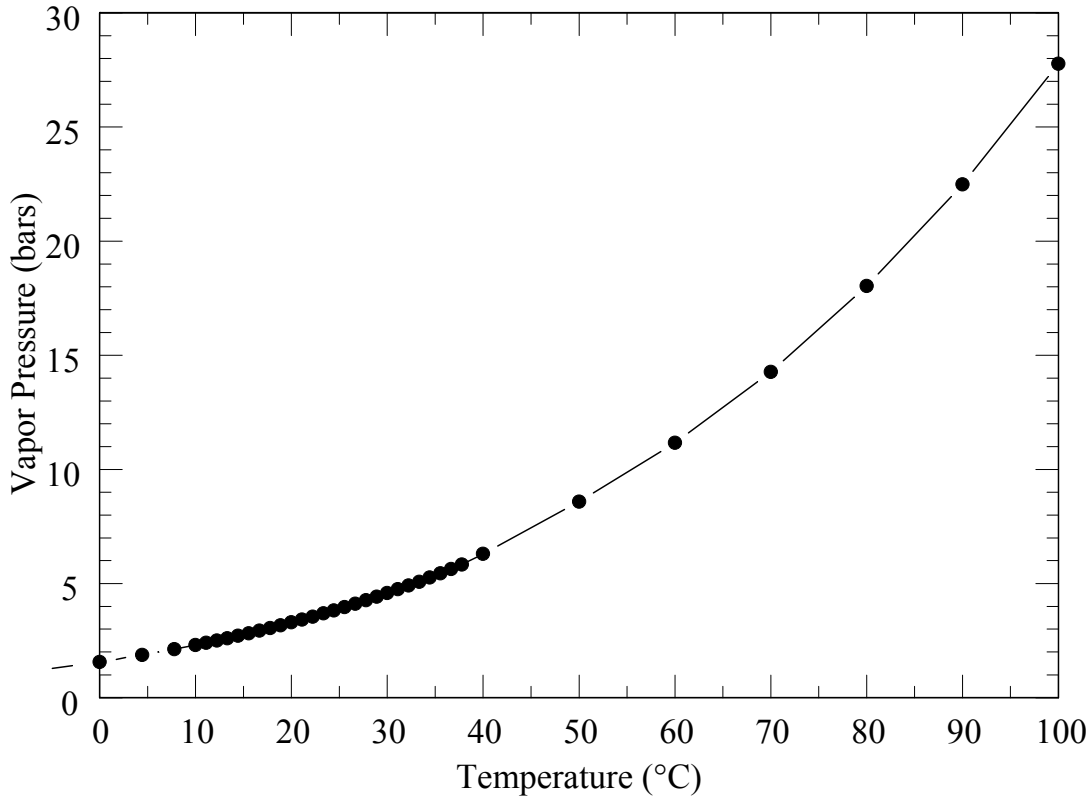


Figure 10. Vapor pressure of sulfur dioxide (Weast, 1988; Vargaftik, 1975).

For comparison, the theoretical limit of acid conversion is given by equilibrium. This limit can be determined as follows. At the decomposer temperature of more than 750 °C, the Gibbs free energy for this reaction $\Delta G_{\text{H}_2\text{SO}_4}$, at this temperature is -48.74 kJ/mol and it decreases further with increasing temperature (HSC5.1, 2002). A negative value for $\Delta G_{\text{H}_2\text{SO}_4}$ indicates that the forward reaction is favored, and because $\Delta G_{\text{H}_2\text{SO}_4}/(RT) = -5.7$, the forward reaction is highly favored. Thus acid vapor is nearly all decomposed to SO_3 and H_2O . SO_3 decomposition requires a catalyst, and at equilibrium for ideal gases the partial pressures of SO_3 , SO_2 and O_2 satisfy,

$$\frac{P_{\text{O}_2}^{1/2} P_{\text{SO}_2}}{P_{\text{SO}_3}} = \exp\left[-\frac{\Delta G_{\text{SO}_3}}{RT}\right], \quad (5)$$

where

ΔG_{SO_3} = Gibbs free energy of reaction of SO_3 to SO_2 and $\frac{1}{2}\text{O}_2$,

R = ideal gas constant, 8.3144 J/(K mol),

T = decomposer temperature, and

P_i = partial pressure of species i .

The total pressure is the sum of all the partial pressures, and is therefore given by,

$$P = P_{\text{SO}_2} + P_{\text{SO}_3} + P_{\text{O}_2} + P_{\text{H}_2\text{O}}. \quad (6)$$

In these tests, the pressure-setting valve determines P . If SO_2 and O_2 are not initially in the system and are generated only by the decomposition of SO_3 , then by stoichiometry,

$$P_{\text{SO}_2} = 2P_{\text{O}_2}. \quad (7)$$

Similarly, if only pure acid is injected, then the partial pressure of water must be equal to sum of partial pressures of SO_2 and SO_3 , since by stoichiometry for each mole of sulfur, there is one mole of water. Because the acid is generally in solution with water, we can define γ as the ratio of moles of water to sum of the moles of SO_2 and SO_3 . For pure acid $\gamma = 1$, but for example if the acid is at a concentration of 80 mol%, then $\gamma = (8+2)/8 = 1.25$, because for 8 moles of acid injected, 2 moles of water are also injected and 8 moles of water form by the decomposition of 8 moles of acid. The value of γ is given for each test in Table 3, and is readily calculated as the inverse mole fraction. By stoichiometry,

$$P_{\text{H}_2\text{O}} = \gamma \left(P_{\text{SO}_2} + P_{\text{SO}_3} \right). \quad (8)$$

Equations (5)-(8) can be combined into a single cubic equation given by,

$$x^3 - \left[\frac{(3+2\gamma)^2 E^2}{4P(1+\gamma)^2} \right] x^2 + \left[\frac{(3+2\gamma)E^2}{2P(1+\gamma)^2} \right] x - \left[\frac{E^2}{4P(1+\gamma)^2} \right] = 0 \quad (9)$$

where we have defined,

$$x \equiv \frac{P_{\text{O}_2}}{P} \leq 0.2 \quad (10)$$

and

$$E \equiv \exp\left[-\frac{\Delta G_{\text{SO}_3}}{RT}\right]. \quad (11)$$

Eq. (9) is readily solved analytically, and then by back-substitution all the partial pressures can be determined. The theoretical maximum conversion occurs at equilibrium and is given by,

$$\eta_t \equiv \frac{P_{\text{SO}_2}}{P_{\text{SO}_2} + P_{\text{SO}_3}} = \frac{2x(1+\gamma)}{1-x}. \quad (12)$$

From Eq. (12) we see that back-substitution is not needed to determine the theoretical maximum conversion, only the solution for x from Eq. (9) and the initial liquid acid concentration are required. In this work, the value of ΔG_{SO_3} was obtained from the HSC 5.1 computer code (2002), and is plotted in Figure 11. The theoretical conversions for the tests are presented along with the measured conversion.

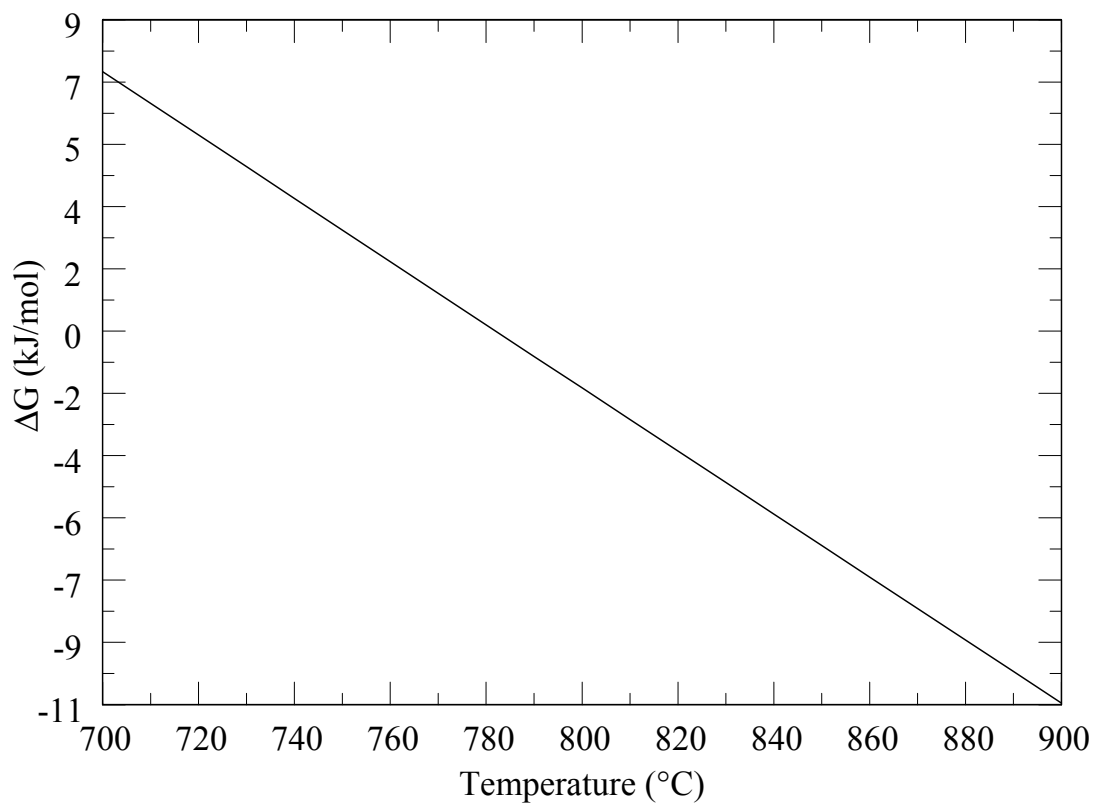


Figure 11. Gibbs free energy of reaction of SO_3 to SO_2 and $\frac{1}{2} \text{O}_2$ per mole of SO_3 reacted, (HSC 5.1 computer code, 2002).

IV. Test Results

The data set for each experiment is large, and therefore several plots have been made for each test. As a guide to the plots, in Table 4 the Figure numbers are given for the type of data available for each test. To concentrate on the data needed to determine η , the data are presented primarily over the time span in which acid was injected. The first plot for a test is the temperature of the boiler. The boiler outlet temperature is displayed which should be significantly above the boiling point of acid to ensure complete vaporization. In addition, the temperature near the acid injection tube at the top of the boiler should also be above the acid boiling point to ensure that hot liquid acid does not corrode the interior side of the top flange. The second plot for a test is the temperature in the decomposer. In particular, the temperature of the catalyst is needed in Eq. (3) to determine the acid conversion fraction. The third plot is a comparison of the stream temperatures exiting the decomposer and entering the condenser. This plot in all the tests demonstrated that the fluid was rapidly quenched from over 400 °C to typically less than 30 °C. The fourth plot provides more detail on the condenser temperature to show that just past the entry region of the condenser, the fluid continued to rapidly cool to below 20 °C. The fifth plot per test displays the system pressure and gas flow rate. In general, the system pressure remained nearly constant at the set pressure throughout the acid pumping phase of the test. Finally, the sixth plot for a test provides the acid conversion fraction for the system pressure and the catalyst temperature. Each point in the sixth plot is computed by averaging five consecutive temperatures from thermocouple number 10 for the abscissa, and the average of five gas flow rates for the same time period for the ordinate. Only temperature and flow data when the set pressure (i.e. 2, 6, or 11 bars) had been achieved are used.

Table 4. Figure index numbers for plots.

Plot	Data Displayed	Figure numbers for test at 2 bars	Figure numbers for test at 6 bars	Figure numbers for test at 11 bars
1	Boiler temperatures	12	18	24
2	Decomposer temperatures	13	19	25
3	Rapid quench check	14	20	26
4	Condenser temperatures	15	21	27
5	Gas flow rates & for tests at 6 and 11 bars system pressure	16	22	28
6	Acid conversion fraction	17	23	29

IV.1. Pressurized Acid Test #1

This preliminary pressurized acid test was designed to assess the equipment and operations. Therefore, only a pressure of 1 bar above ambient was adequate for evaluating the equipment and instrumentation. Two previous tests were run with deionized water instead of acid, and for those tests, all the instrumentation worked well without problems. However, on the day of the test prior to acid injection, the gas chromatograph (GC) indicated that the oxygen concentration in air had dropped from about 21% to less than 10%, and the instrument could only identify 90% of the gases in air. Prior to moving the GC to the test site, 100% of the calibration gas mixtures were correctly identified. The discrepancy on the day of the test was attributed to a possible error in the parameter settings for evaluating the elution curves. These curves are stored on the computer and can thus be reevaluated later with different parameter settings. Servicing the GC takes about two weeks, which would have delayed the tests. GC data are primarily a check on the gas composition, and are not required for determining the acid conversion fraction. For these reasons, and because elution curve data would still be available, we decided to proceed even without complete confidence that there would be reliable gas composition data. As discussed later, the technical difficulties with the GC became worse and for the third test of this series, for some measurements the GC did not identify more than 50% of the effluent gas.

The heat up phase started at 12:53 and by 16:19 the bypass valve was closed and acid injection began. As can be seen from Figure 12, the boiler temperature at the center was stable throughout the acid injection period. More importantly, after acid was introduced, the temperature drop inside the boiler did not reduce the inside temperature below 400 °C, and therefore all the acid should have quickly vaporized long before reaching the much hotter boiler walls. The acid exiting the boiler was well above 600 °C throughout the test, and increased to about 700 °C by the end of acid injection. This increase in outlet temperature was observed in all three tests.

We noted that thermocouple number 4, which was used to control the boiler heater was somewhat noisy. Similarly, as shown in Figure 13, thermocouple number 9 that was used to control the decomposer heater was also noisy. Only thermocouples that were split for both data recording and heater controls had significant noise. The noise on both these thermocouples persisted for all three tests. In future tests, two separate thermocouples at the same location will be used for these two applications. Because there was another thermocouple (10) in the catalyst bed, for these tests we did not spend time to disassemble the heaters, route an additional thermocouple, and then reassemble the heater.

The decomposer temperatures shown in Figure 13 had a curious oscillation of about 30 °C with a period of about 8 minutes. Because the oscillation was common to all the decomposer thermocouples, it was obvious that the heater controller was malfunctioning. The problem was readily found and corrected by reprogramming this controller and the oscillation pattern did not reappear in subsequent tests. Unfortunately, because the acid conversion fraction is dependent on the catalyst temperature, we did not attain a steady temperature for the calculated value of η , the acid conversion fraction computed from Eq. (3). As discussed later, the temperature oscillation probably contributed significantly to the scatter in η for this test.

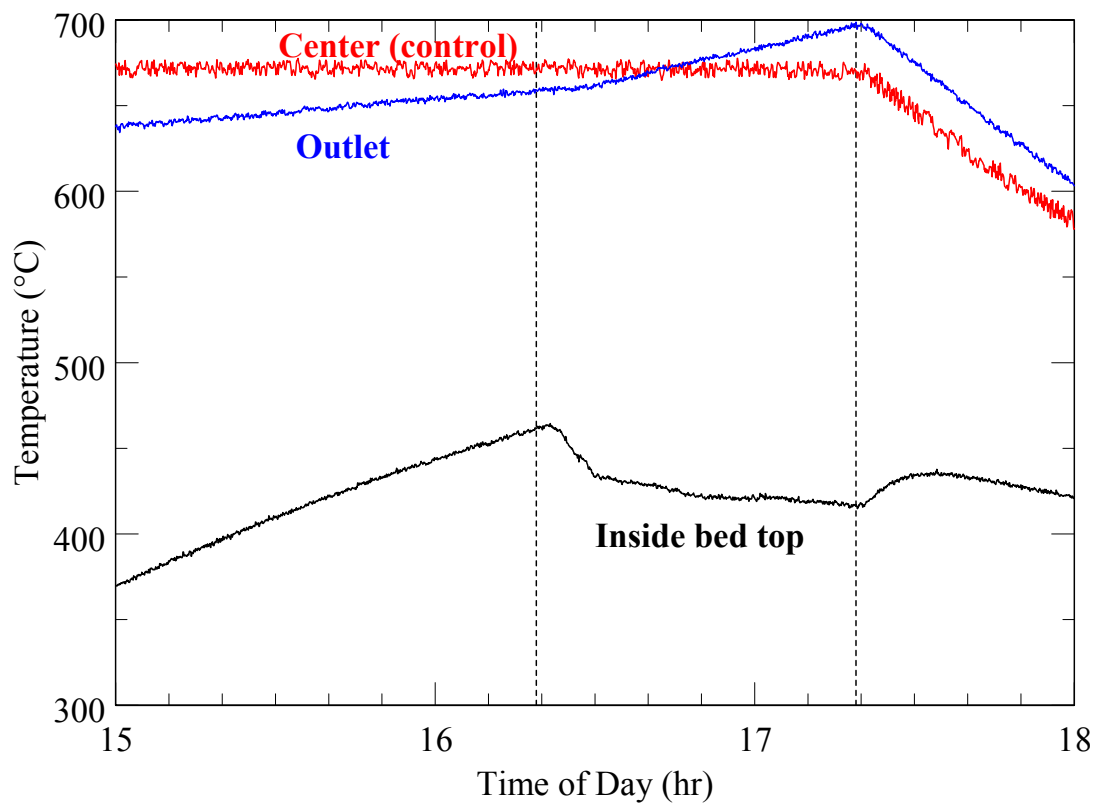


Figure 12. Boiler temperatures for pressurized acid test #1 at 2 bars performed on 7 July 2005. The curves labeled “Inside bed top”, “Center”, and “Outlet” correspond to thermocouples numbered 1, 4, and 5, respectively, in Table 1. The vertical broken lines on the left and right correspond to the times at which the acid pump was turned on and off, respectively.

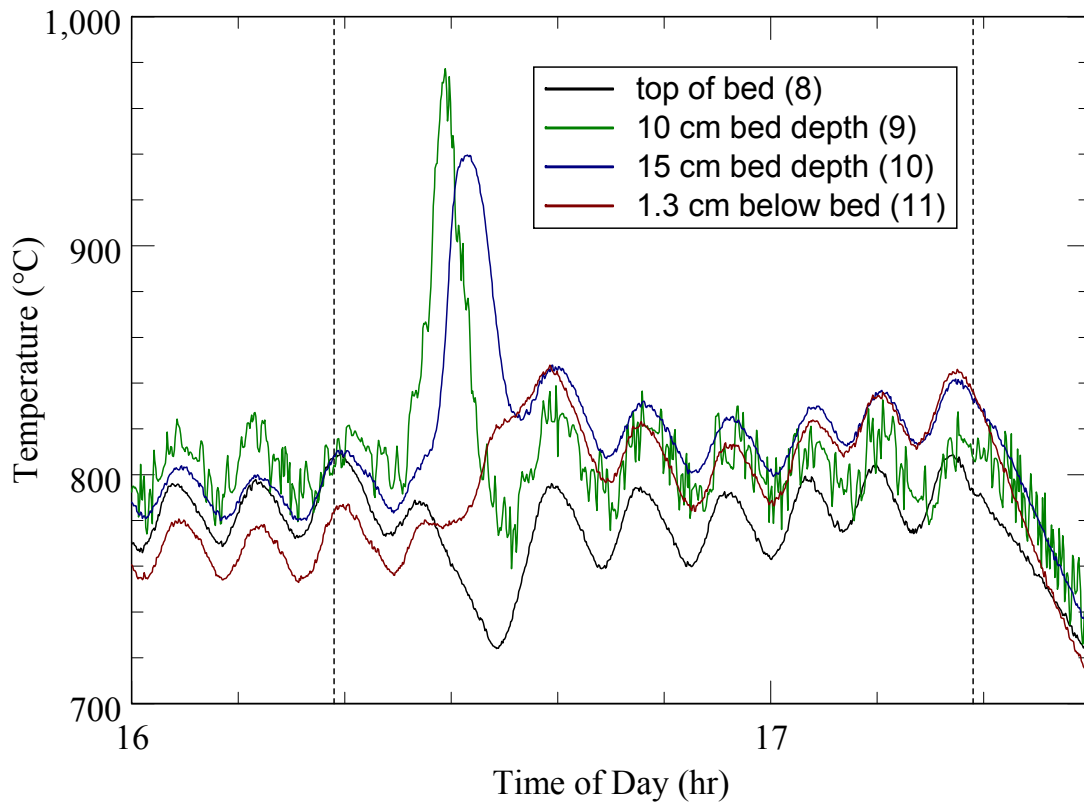


Figure 13. Decomposer temperatures for pressurized acid test #1 at 2 bars performed on 7 July 2005. The numbers in parentheses in the legend correspond to the thermocouple numbers in Table 1. The oscillation was due to an incorrect heater controller setting, which was corrected in subsequent tests. The vertical broken lines on the left and right correspond to the times at which the acid pump was turned on and off, respectively.

A great concern was the rapid increase in catalyst temperature (at thermocouple 9) to almost 1000 °C soon after acid injection started. This excursion was also observed on the adjacent downstream thermocouple (10), but the temperature at the upstream thermocouple (8) decreased during this excursion. These results seem to indicate that an exothermic reaction may have occurred, possibly with a contaminant when acid first contacted the catalyst bed. Because the excursion was not observed again, the contaminant hypothesis seems reasonable, but further work is required to confirm this hypothesis.

Based on the temperatures shown in Figure 14, it is clear that the acid vapors at the bottom of the decomposer were rapidly quenched inside the condenser to less than 50 °C. In Figure 15, the temperature range is smaller, and from this Figure the stream temperature in the condenser was reduced further to about 10 °C. Thus the data supports the assumption that nearly all the acid and water vapor were condensed into the collection flask.

In Figure 16 the gas flow rate has a lag of about 5 minutes from the time acid injection started before the rate increased rapidly. This lag was probably due to the time required for pressure buildup. During the first 20-minute period of acid injection there was a temperature excursion that probably resulted in the initial large gas flow rate of about 2 liters/minute. The flow rate decreased to a minimum at about 16:50 and then increased for the remainder of the acid injection period. The temperature oscillations make it difficult to interpret this second increase in gas flow. In this test, pressure data was not recorded reliably, but the problem was corrected in subsequent tests.

One unintended benefit of the temperature oscillation and excursion is that there is much data on the variation of acid conversion fraction with temperature. Because thermocouple number 8 was upstream of the flow, and thermocouple number 9 was very noisy, thermocouple number 10, which was inserted into the catalyst bed, was used to calculate η . In Figure 17, η has considerable scatter, but shows the expected trend that acid conversion increases with increasing temperatures.

The first pressurized acid test served the purpose of “weeding out” problems before proceeding with the more important tests at the higher pressures of 6 and 11 bars, which is in the range anticipated for the SI (Sulfur-Iodine) cycle. Two problems that were discovered were the oscillating heater control, and lack of computer storage of data from the pressure transducer. Both of these were resolved for tests 2 and 3. At the end of the first test a review of the gas chromatograph data was encouraging because the SO₂ and O₂ concentrations were fairly steady at 58% and 30%, respectively. This is very close to the expected two-to-one ratio of the SO₂ to O₂ for acid decomposition. But the total gas concentration was still below 90%, and in a subsequent review there were no other peaks in the elution curve that would correspond to N₂, H₂, CO₂, or H₂S. As discussed earlier, the problem with the GC was not serious enough to delay the next two tests.

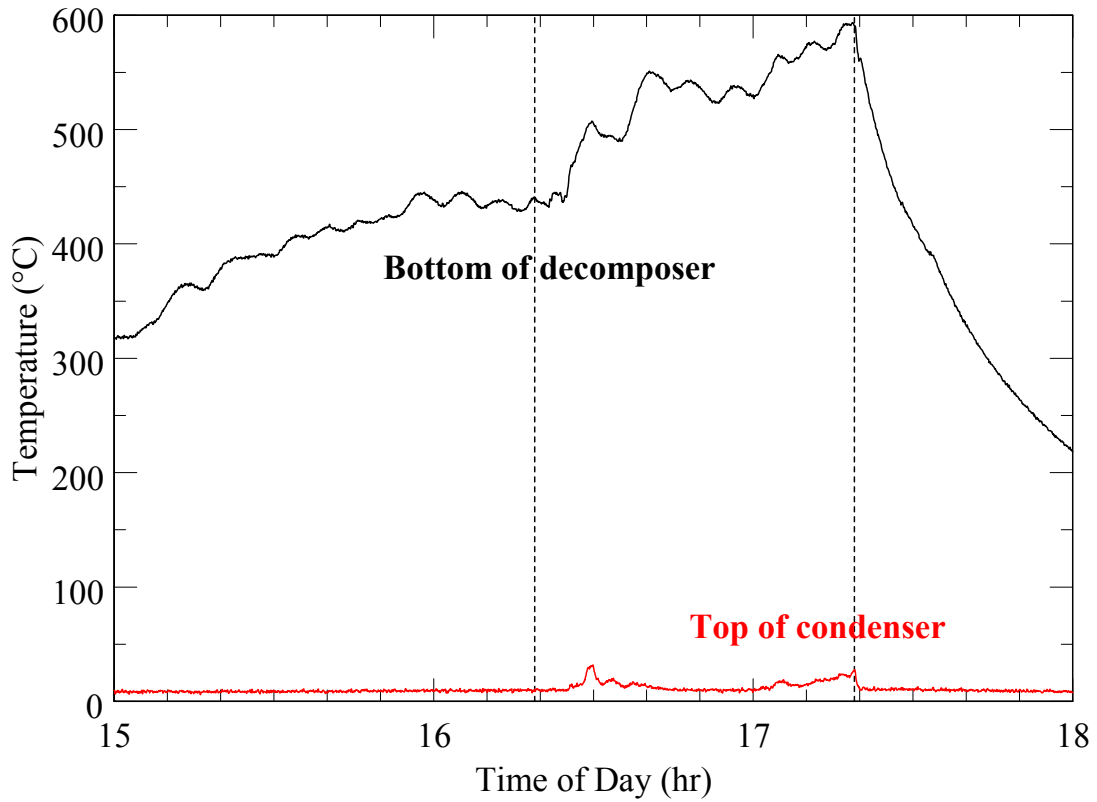


Figure 14. Rapid quenching of fluid from decomposer to condenser for pressurized acid test #1 at 2 bars performed on 7 July 2005. The curves labeled “Bottom of decomposer” and “Top of condenser” correspond to thermocouples numbered 13 and 14, respectively in Table 1. The vertical broken lines on the left and right correspond to the times at which the acid pump was turned on and off, respectively.

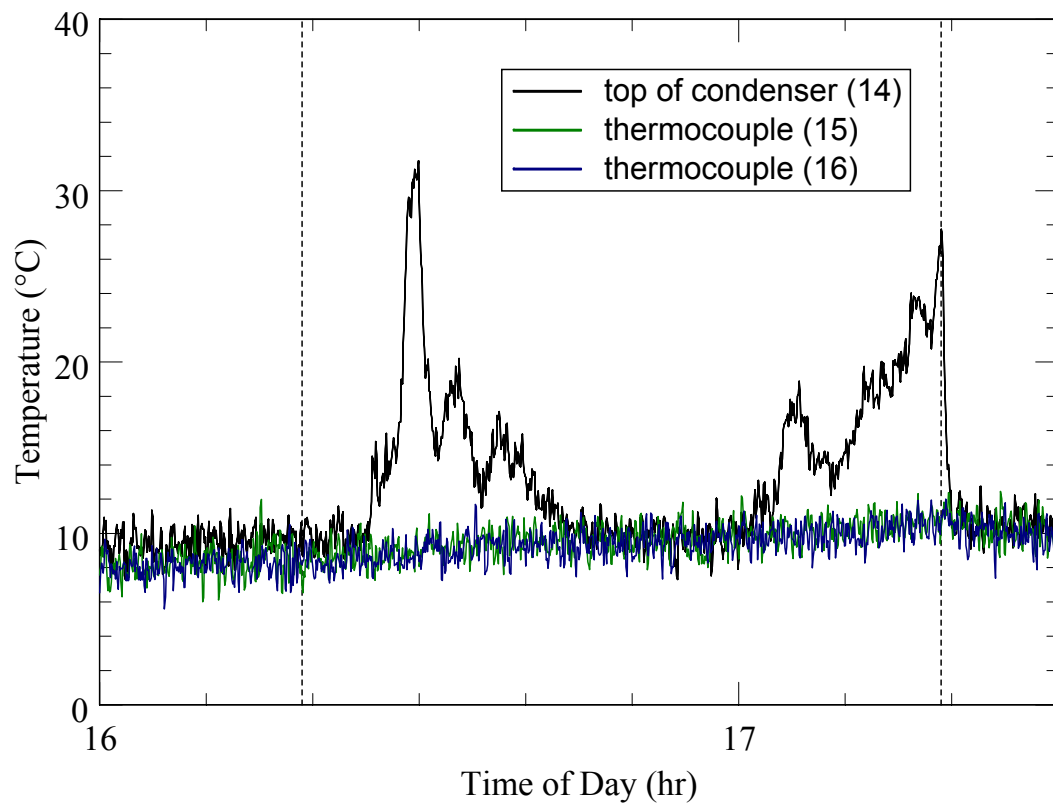


Figure 15. Condenser temperatures for pressurized acid test #1 at 2 bars performed on 7 July 2005. The numbers in parentheses in the legend correspond to the thermocouple numbers in Table 1. The vertical broken lines on the left and right correspond to the times at which the acid pump was turned on and off, respectively.

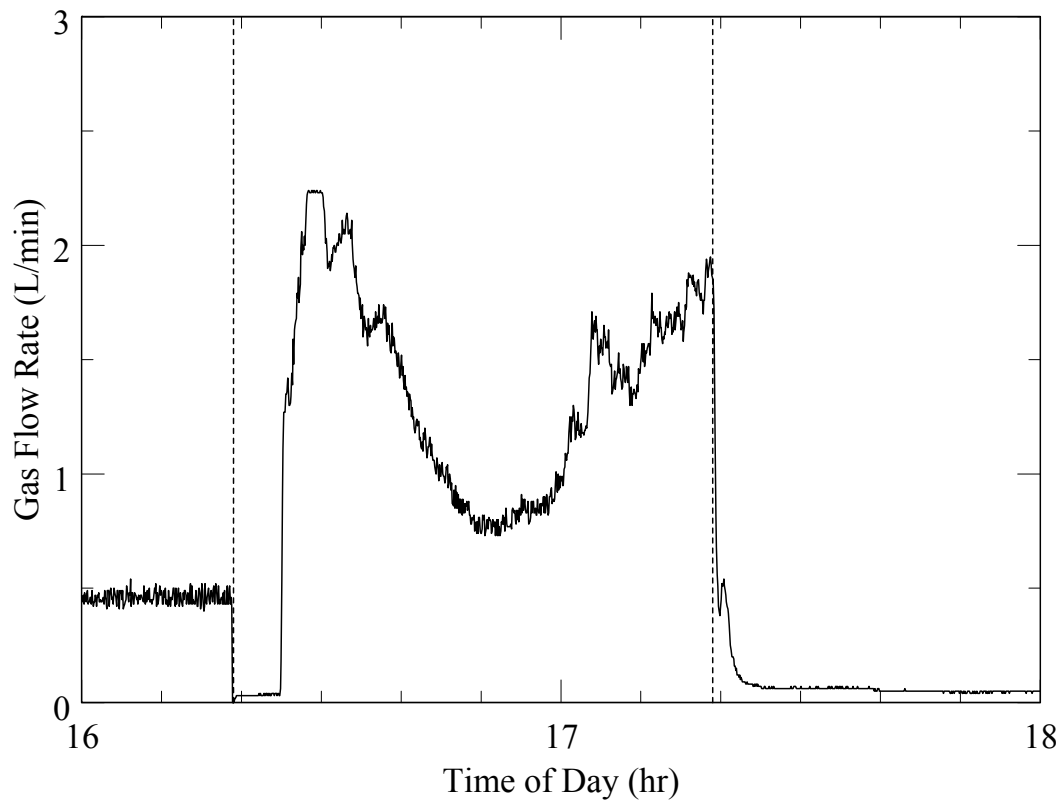


Figure 16. Total gas flow rate of effluent for pressurized acid test #1 at 2 bars performed on 7 July 2005. The pressure was not recorded for this test. The vertical broken lines on the left and right correspond to the times at which the acid pump was turned on and off, respectively.

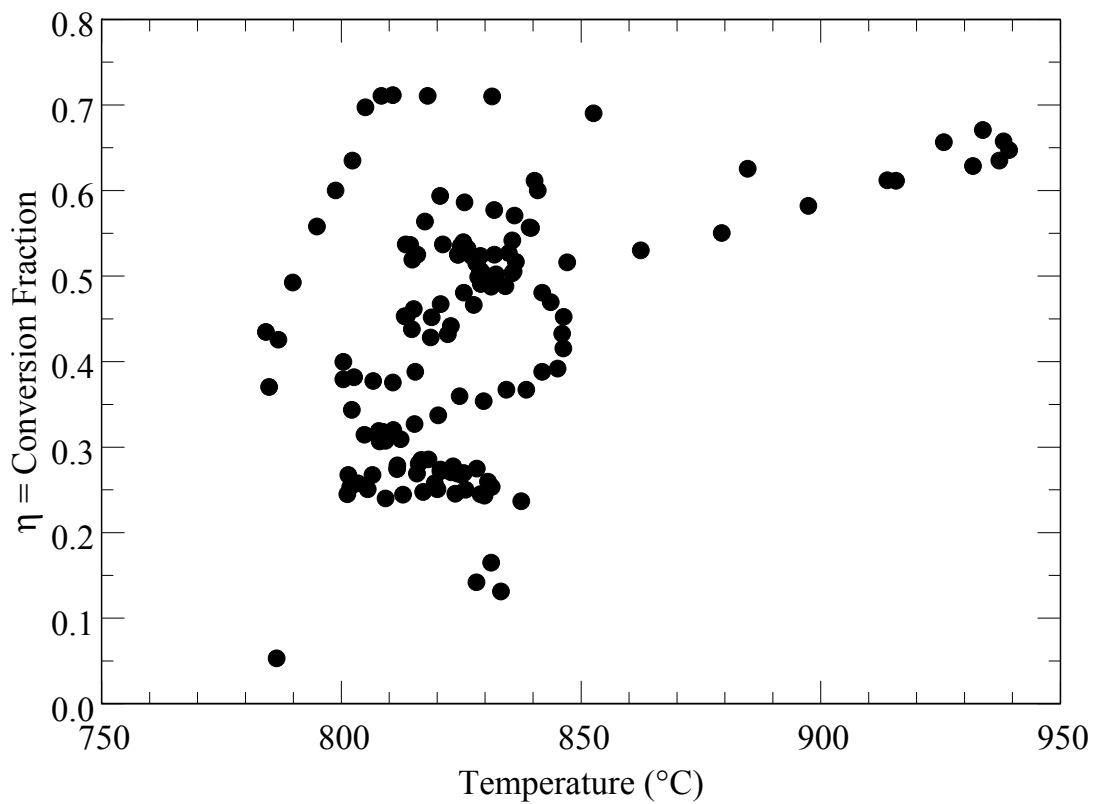


Figure 17. Acid conversion fraction for pressurized acid test #1 at 2 bars performed on 7 July 2005. The temperature is that measured by thermocouple number 10, which was inserted into the catalyst bed. Experimental problems that caused the large scatter in this data set were corrected in subsequent tests.

IV.2. Pressurized Acid Test #2

Acid injection for the second test began at 12:59 on 18 July 2005. As can be seen from Figure 18, the boiler temperature at the center was stable and cold liquid acid injection did not reduce the inside temperature significantly below 400 °C. The acid exiting the boiler was again well above 600 °C throughout the test.

At this higher pressure of 6 bars, there was concern that if another temperature excursion occurred the apparatus would fail structurally at 1000 °C. Because metal strength decreases with increasing temperature, the starting temperature of the decomposer was reduced to about 750 °C from 800 °C. This change in starting temperature can be seen by comparing Figures 13 and 19. As can be seen from Figure 19, no temperature excursion occurred. Nonetheless, this cautious approach had some unintended consequences that almost terminated the test prematurely.

For this experiment, the pressure was recorded and from Figure 22 we see that after about 12 minutes from the start of acid injection, the pressure reached the desired level of about 6 bars. However, no gas flow was measured at the time, and there was great concern that the gas flow meter had failed. This suspicion was confirmed by the high levels of SO₂ and O₂ from the GC. Thus, gas had to have been released from the system if the acid pump was injecting acid and a high concentration of SO₂ was observed. If the flow meter had failed, the acid conversion fraction could not be calculated. Because the system was pressurized, we could not safely approach the apparatus to check the flow meter. After some discussions in the control room, we decided to open the bypass valve and shut down the acid pump. This would provide a rapid rush of gas to the flow meter, which would register if it was working properly. Alternatively, if no flow pulse was measured then the flow meter was defective and the test would be stopped. If the meter was defective, then once the system was depressurized and acid flow had stopped, we could inspect the flow meter. As can be seen in Figure 22, the gas flow rate pulsed upwards exactly when the pressure dropped due to the opening of the bypass valve at 13:25. Thus, the flow meter seemed to be operating and acid pumping resumed at 13:30. Apparently, the lower decomposer temperature significantly reduced the conversion fraction and the small amount of gas pushed out of the apparatus was due to the liquid volume of acid displacing some of the SO₂ formed in the decomposer. However, at the low temperature of ~750 °C there was negligible acid conversion, which was not expected based on previous work (General Atomics, 1986).

Because the temperature excursion did not occur, it was safe to raise the decomposer temperature to 775 °C. This is shown in Figure 19. At this higher temperature, a measurable gas flow was generated as can be seen in Figure 22 at 13:43. Comparing Figures 19 and 13 it is clear that the temperature oscillations in the decomposer had been resolved. To obtain conversion data at several temperatures, the decomposer temperature was increased in a series of three steps to about 850 °C. As shown in Figures 20 and 21, throughout this period the condenser was able to rapidly quench the hot vapors from the decomposer. The one spike in temperature above the boiling point of water, 159 °C (at 6 bars), in the top thermocouple in the decomposer may have been due to some acid droplets impacting the thermocouple well. Nonetheless, from Figure 21 we can see that the decomposer was generally at a temperature of less than 20 °C.

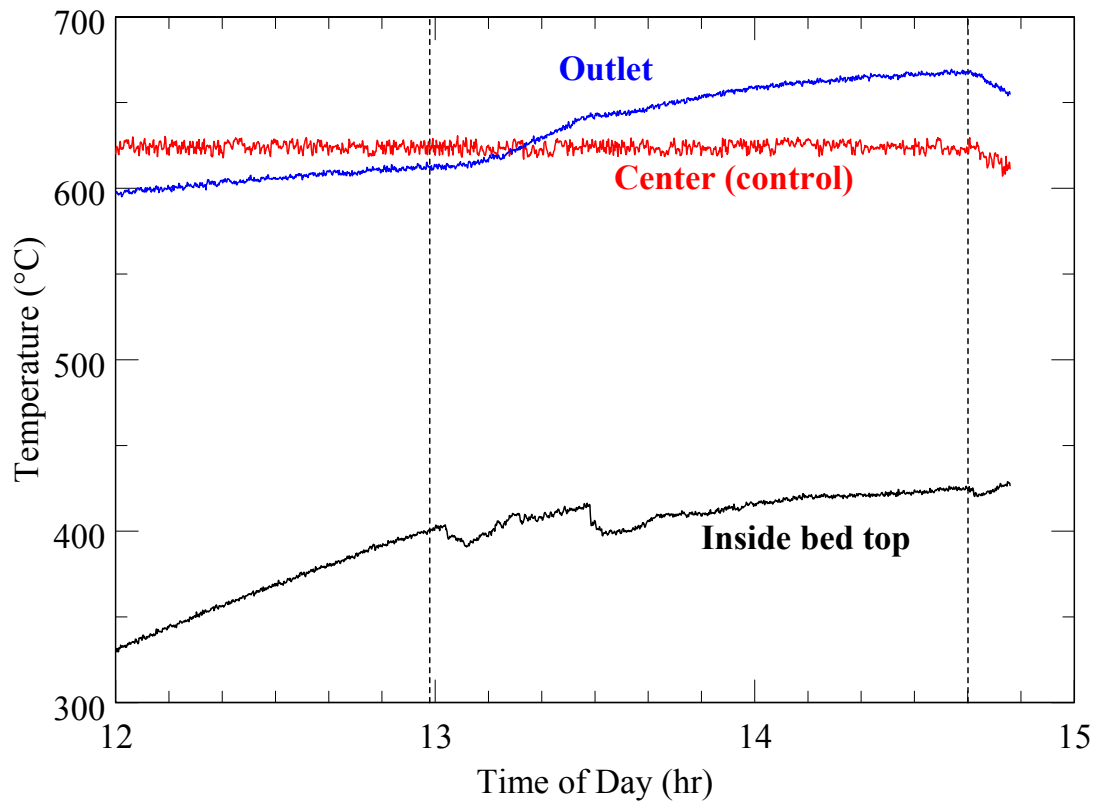


Figure 18. Boiler temperatures for pressurized acid test #2 at 6 bars performed on 18 July 2005. The curves labeled “Inside bed top”, “Center”, and “Outlet” correspond to thermocouples numbered 1, 4, and 5, respectively, in Table 1. The vertical broken lines on the left and right correspond to the times at which the acid pump was turned on and off, respectively.

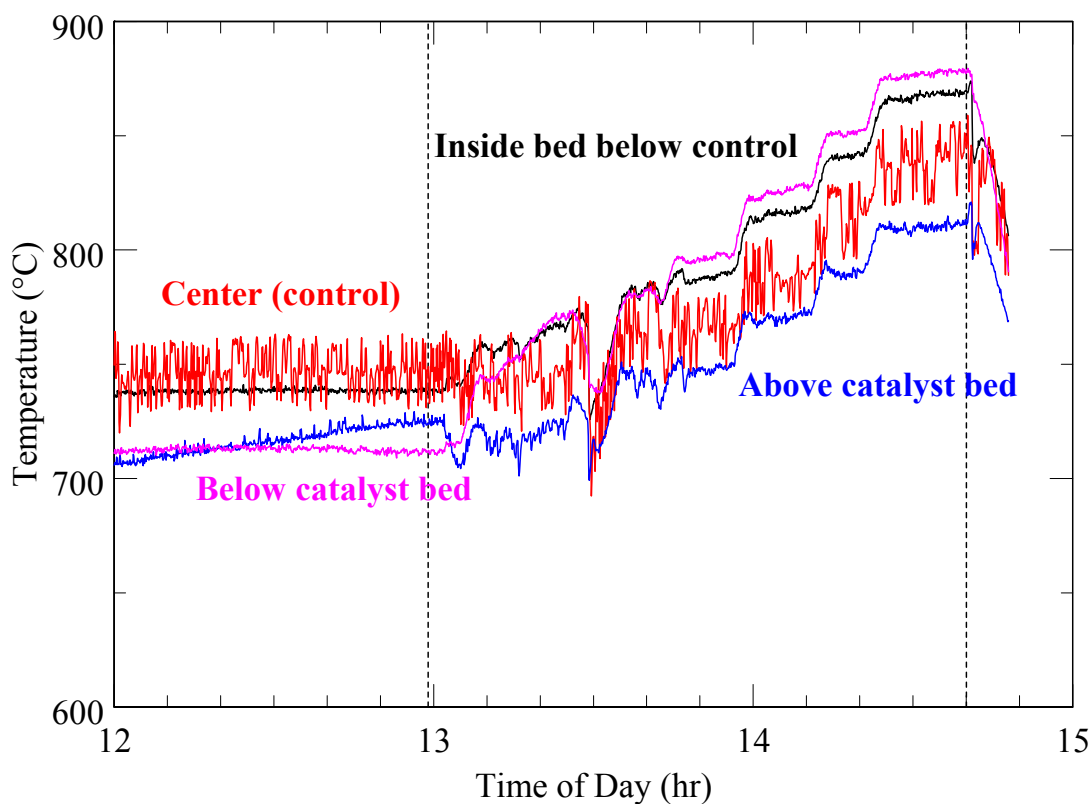


Figure 19. Decomposer temperatures for pressurized acid test #2 at 6 bars performed on 18 July 2005. The curves labeled “Above catalyst bed”, “Center”, and “Inside bed below control”, and “Below catalyst bed” correspond to thermocouples numbered 8, 9, 10, and 11, respectively in Table 1. The vertical broken lines on the left and right correspond to the times at which the acid pump was turned on and off, respectively.

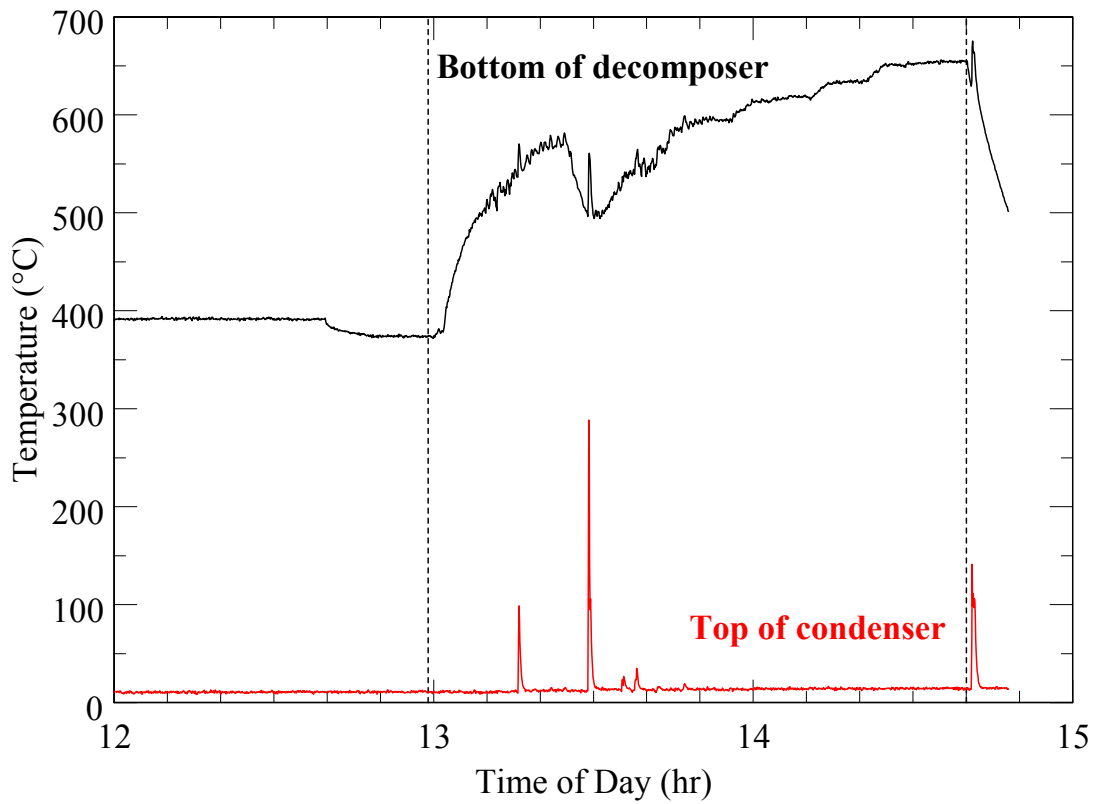


Figure 20. Rapid quenching of fluid from decomposer to condenser for pressurized acid test #2 at 6 bars performed on 18 July 2005. The curves labeled “Bottom of decomposer” and “Top of condenser” correspond to thermocouples numbered 13 and 14, respectively in Table 1. The vertical broken lines on the left and right correspond to the times at which the acid pump was turned on and off, respectively.

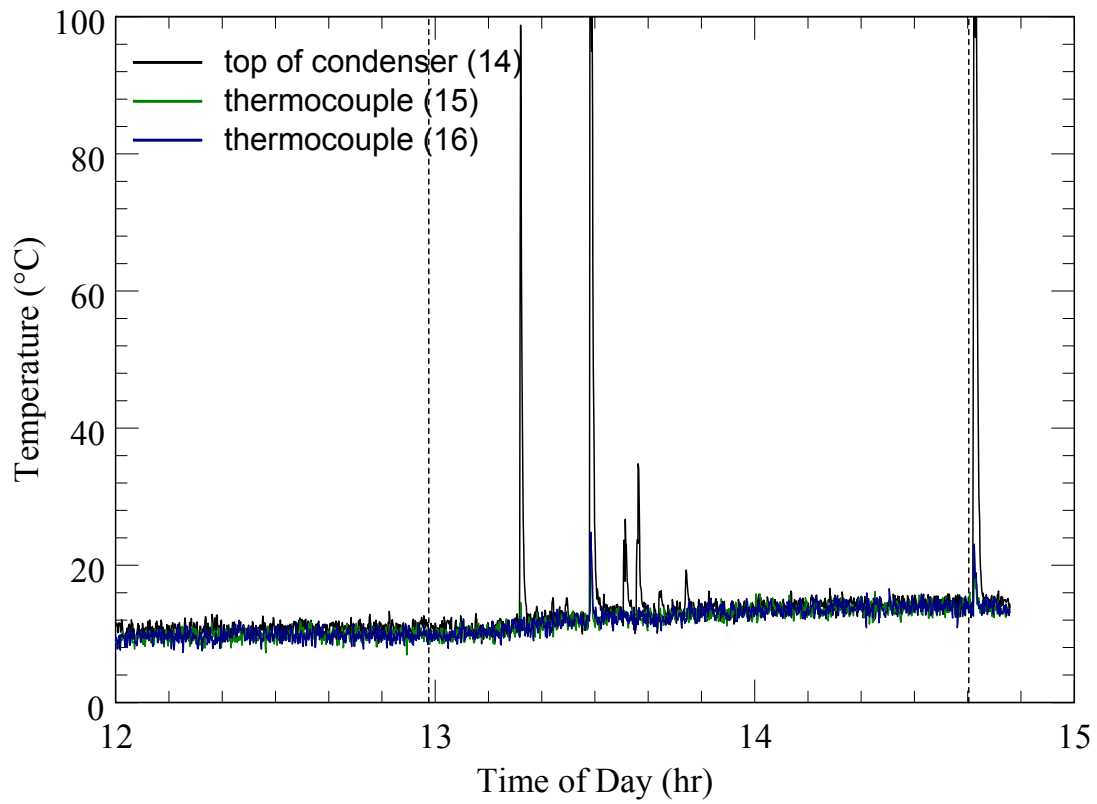


Figure 21. Condenser temperatures for pressurized acid test #2 at 6 bars performed on 18 July 2005. The numbers in parentheses in the legend correspond to the thermocouple numbers in Table 1. The vertical broken lines on the left and right correspond to the times at which the acid pump was turned on and off, respectively.

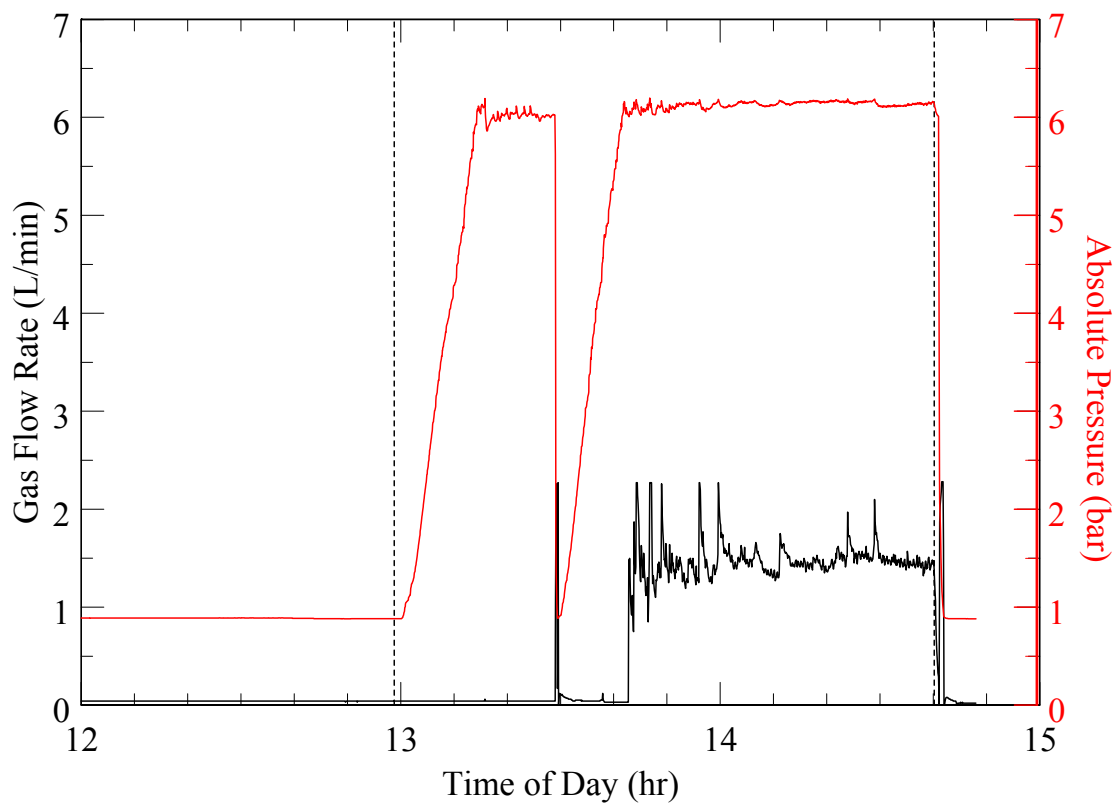


Figure 22. Total gas flow rate of effluent and system pressure for pressurized acid test #2 at 6 bars performed on 18 July 2005. The vertical broken lines on the left and right correspond to the times at which the acid pump was turned on and off, respectively.

From Figure 22 we see that at times there was a rapid variation in the flow rate. This may have been due to a sticking and rapid releasing of the diaphragm in the pressure-relief valve. These abrupt transitions unfortunately introduced scatter into the computed acid conversion fraction. Nonetheless, as can be seen in Figure 23, the scatter in the acid conversion fraction is far less than that introduced by the temperature oscillations in the first test shown in Figure 17. From Figure 23, the acid conversion fraction varied from about 0.4 to 0.45 for the temperature range of 775 °C to 875 °C, respectively. This agrees with the expectation that acid conversion increases with increasing temperature. The conversion data are well bounded by the equilibrium limit computed from Eq. (12) and shown as a line in Figure 23.

The effluent gases identified by the GC were initially 55% SO₂ and 31% O₂. Near the end of the test, the SO₂ and O₂ concentrations were 47% and 40%, respectively. Throughout the test, the GC identified no more than 88% of the gas. As discussed earlier, the GC measurements are suspect. This will be addressed in future experiments with more extensive testing of the instrument prior to running a decomposition experiment.

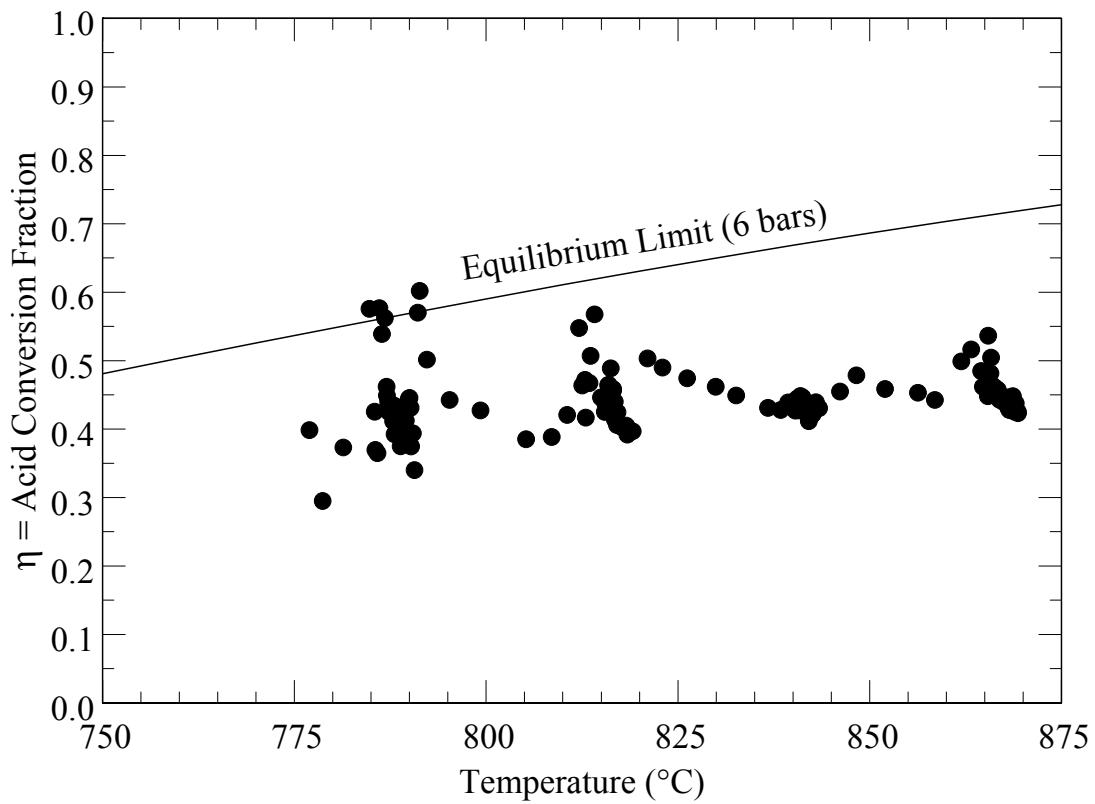


Figure 23. Acid conversion fraction for pressurized acid test #2 at 6 bars performed on 18 July 2005. The temperature is that measured by thermocouple number 10, which was inserted into the catalyst bed.

IV.3. Pressurized Acid Test #3

Acid injection for the third test began at 13:13 on 20 July 2005. As can be seen from Figure 24, the boiler temperature at the center was stable and acid injection did not reduce the inside temperature significantly below 400 °C. The acid exiting the boiler was again well above 600 °C throughout the test.

The decomposer temperature was increased in 25 °C steps from 750 °C to 850 °C, and it was held at each step for half an hour. The stepping of the decomposer temperature can be seen in Figure 25. As shown in Figures 26 and 27, throughout the test the condenser was able to rapidly quench the hot vapors from the decomposer. From Figure 28 we see that the rapid oscillations with the gas flow rate are more problematic than what occurred in the second acid test as shown in Figure 22. The effect of these oscillations was the introduction of scatter into η as shown in Figure 29. The average value of η increased from about 0.3 to 0.5 as the temperature increased from 750 °C to 850 °C. The data in Figures 23 and 29 are plotted in Figure 30. The data are mostly bounded by the theoretical equilibrium-limiting value of η_t as given by Eq. (12) and plotted in Figure 30 as solid lines. The theoretical small decrease in conversion fraction with increasing pressure is not readily discerned from the data, probably due to the scatter in the measurements.

The effluent gases identified by the GC soon after acid injection were less than 4% O₂ and no SO₂, and thus more than 95% of the gas was unidentified. Within 30 minutes from the start of acid injection, the data from the GC were about 38% SO₂ and 10% O₂, which means that more than 50% of the gas was unidentified by the GC. Near the end of the test, the SO₂ and O₂ concentrations were 38% and 49%, respectively, which provides an experimental value of β from Eq. (5) of 0.89. Throughout the test, the SO₂ concentrations varied between 38% and 47%. As discussed earlier, these measurements are highly suspect.

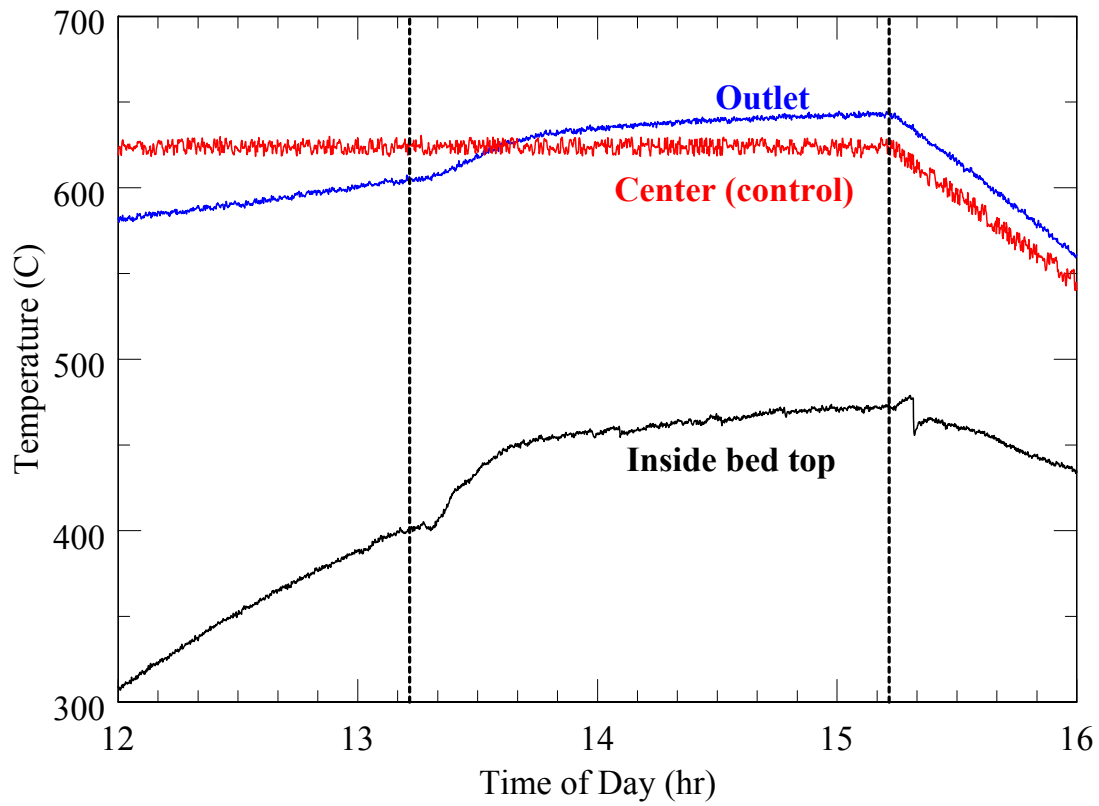


Figure 24. Boiler temperatures for pressurized acid test #3 at 11 bars performed on 20 July 2005. The curves labeled “Inside bed top”, “Center”, and “Outlet” correspond to thermocouples numbered 1, 4, and 5, respectively, in Table 1. The vertical broken lines on the left and right correspond to the times at which the acid pump was turned on and off, respectively.

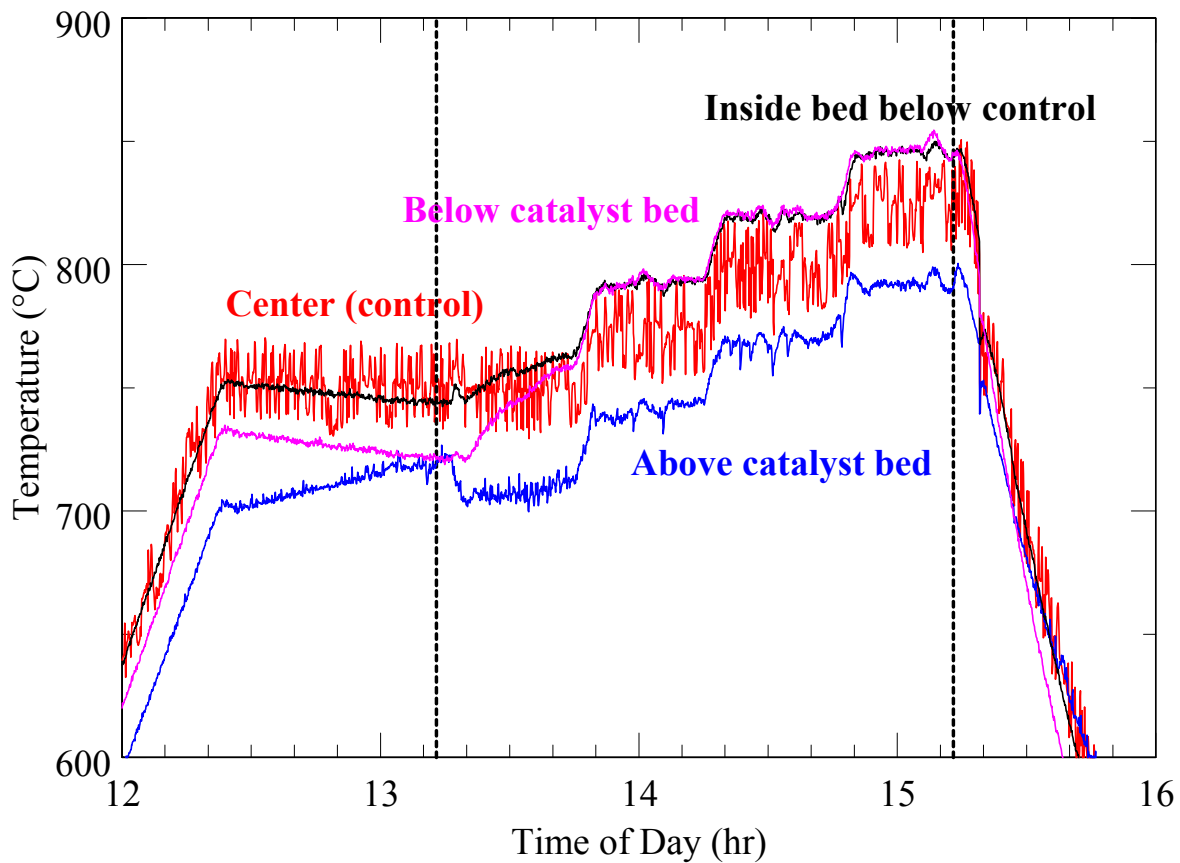


Figure 25. Decomposer temperatures for pressurized acid test #2 at 11 bars performed on 20 July 2005. The curves labeled “Above catalyst bed”, “Center”, and “Inside bed below control”, and “Below catalyst bed” correspond to thermocouples numbered 8, 9, 10, and 11, respectively in Table 1. The vertical broken lines on the left and right correspond to the times at which the acid pump was turned on and off, respectively.

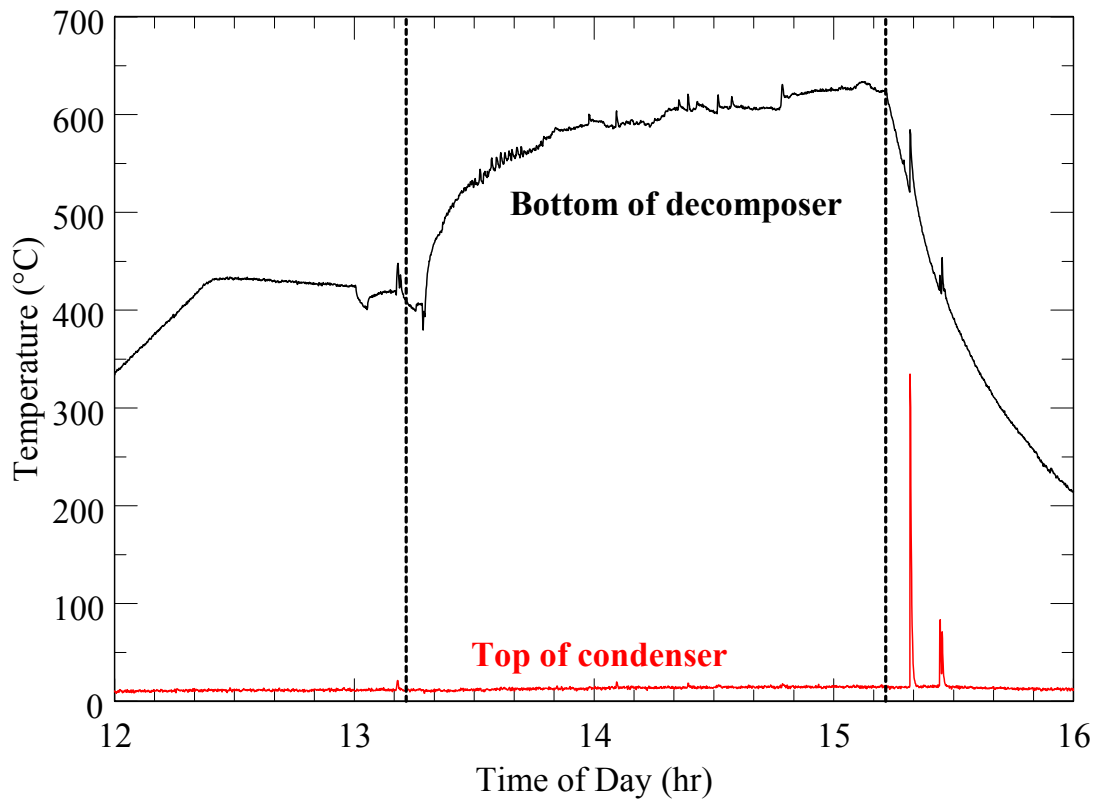


Figure 26. Rapid quenching of fluid from decomposer to condenser for pressurized acid test #3 at 11 bars performed on 20 July 2005. The curves labeled “Bottom of decomposer” and “Top of condenser” corresponds to thermocouples numbered 13 and 14, respectively in Table 1. The vertical broken lines on the left and right correspond to the times at which the acid pump was turned on and off, respectively.

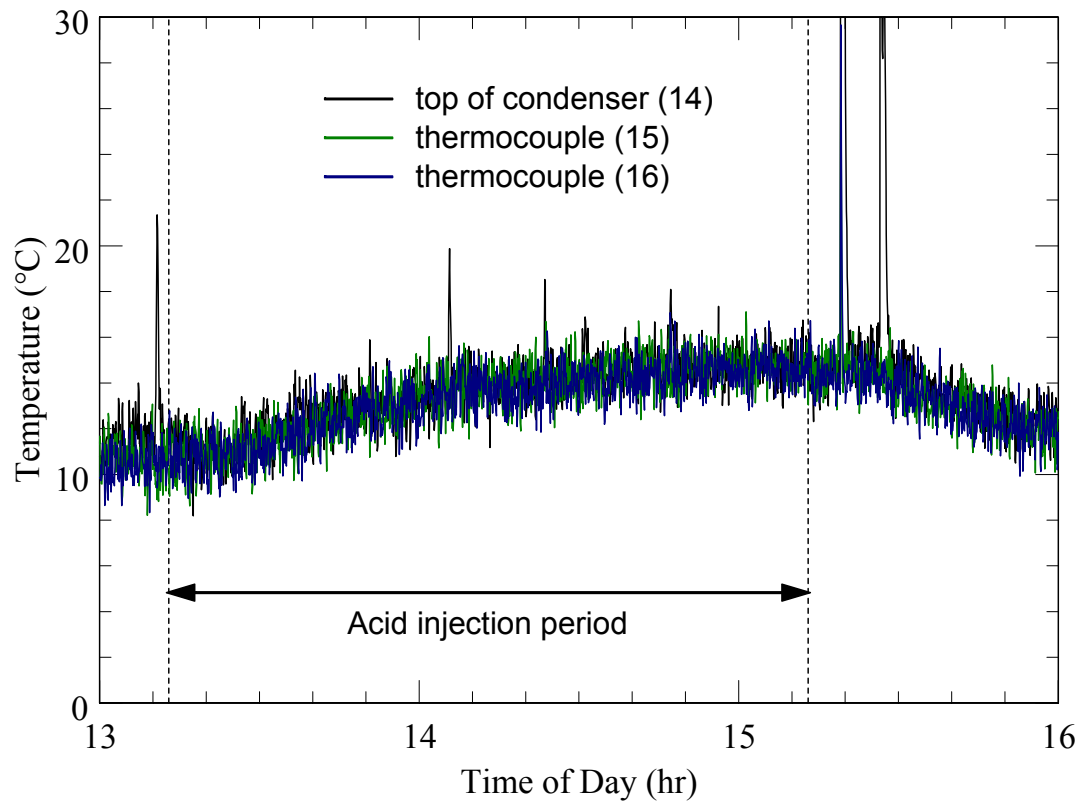


Figure 27. Condenser temperatures for pressurized acid test #3 at 11 bars performed on 20 July 2005. The numbers in parentheses in the legend correspond to the thermocouple numbers in Table 1. The vertical broken lines on the left and right correspond to the times at which the acid pump was turned on and off, respectively.

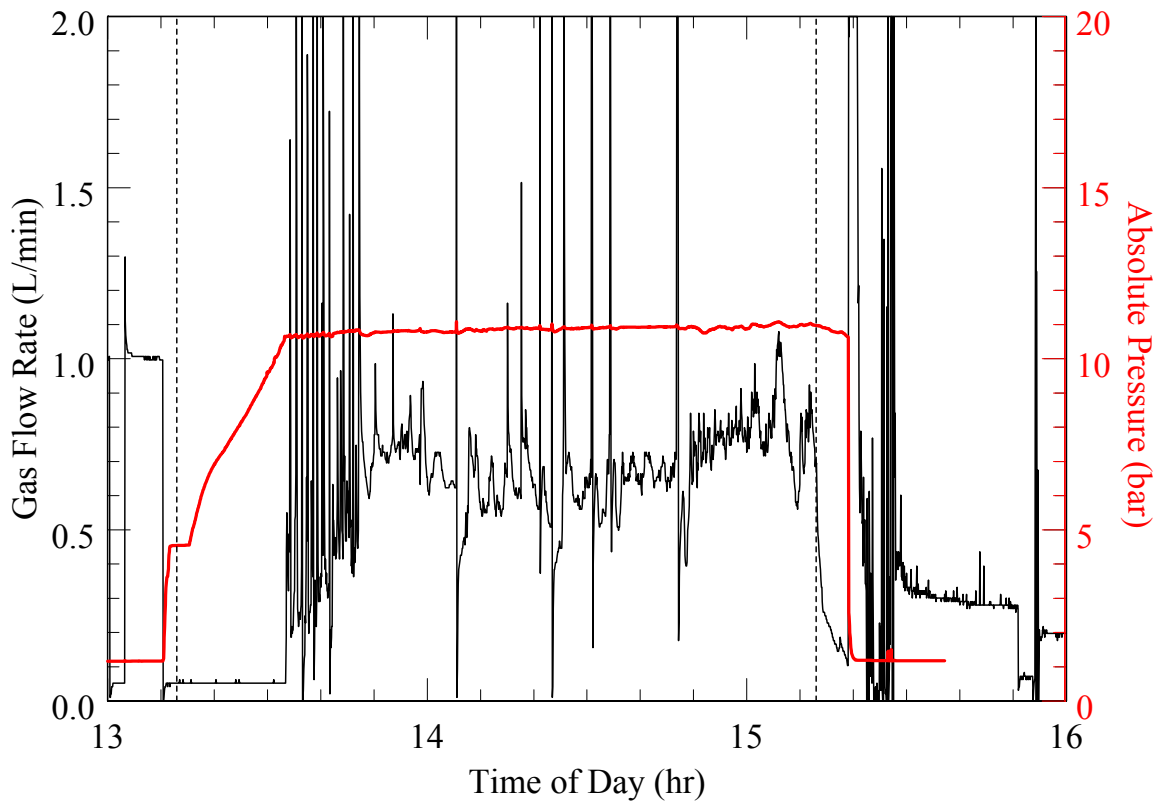


Figure 28. Total gas flow rate of effluent and system pressure for pressurized acid test #3 at 11 bars performed on 20 July 2005. The vertical broken lines on the left and right correspond to the times at which the acid pump was turned on and off, respectively.

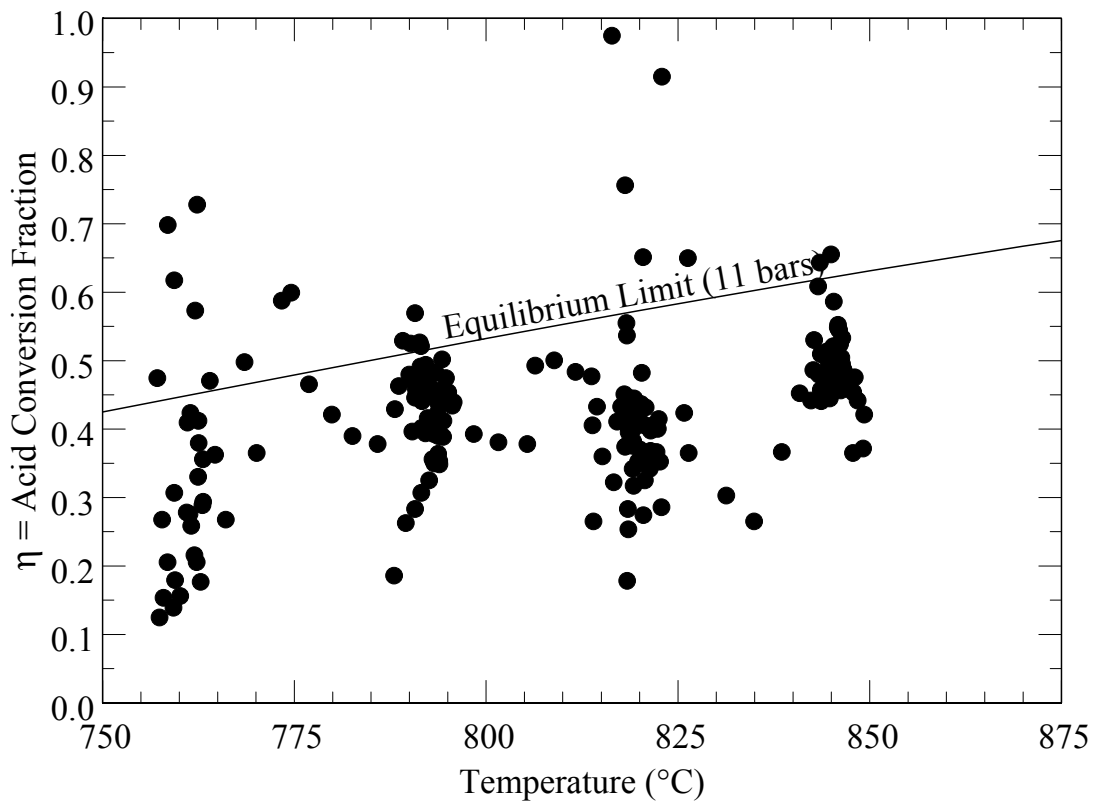


Figure 29. Acid conversion fraction for pressurized acid test #3 at 11 bars performed on 20 July 2005. The temperature is that measured by thermocouple number 10, which was inserted into the catalyst bed.

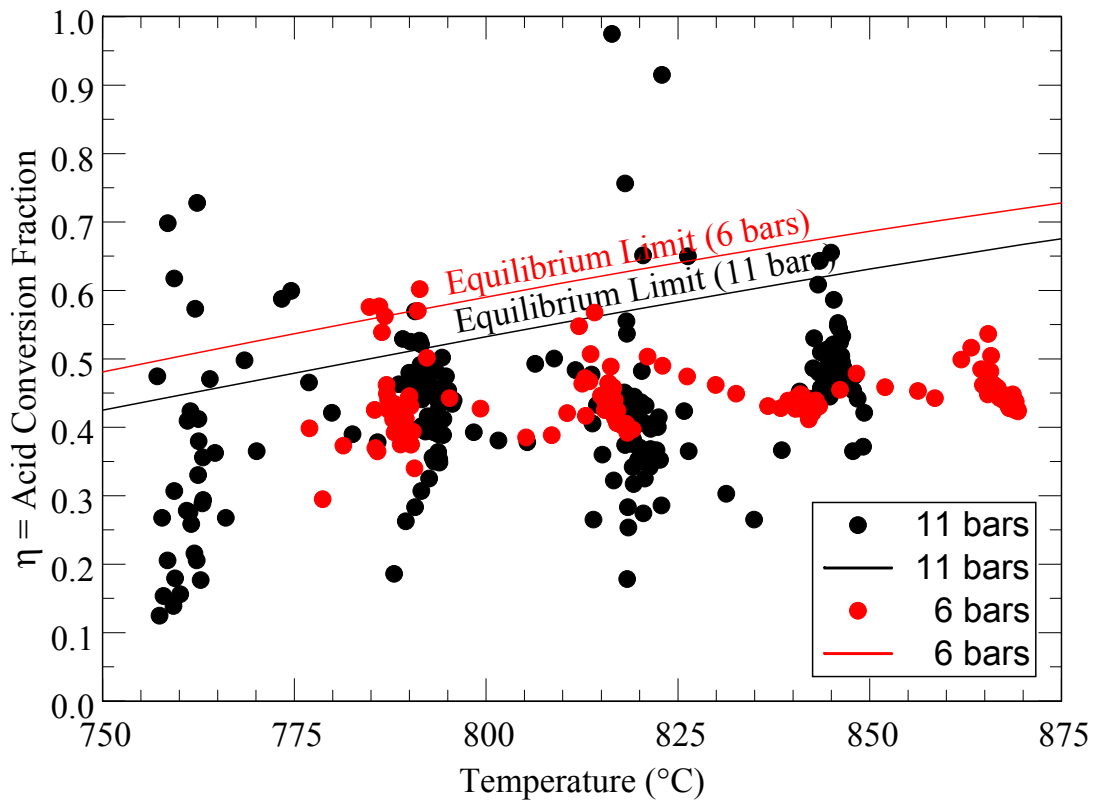


Figure 30. Comparison between conversion fractions at 6 and 11 bars over the temperature range 750 °C to 875 °C. The theoretical equilibrium limit of conversion is computed from Eq. (12).

V. Conclusions

A series of three pressurized sulfuric acid decomposition tests has been completed in support of the Nuclear Hydrogen Initiative thermochemical hydrogen production research program. The tests were performed at absolute pressures of 2, 6, and 11 bars, and for each pressure at temperatures varying between 750 – 875 °C. Because real-time measurements of acid conversion were used for the first time, the measurements of conversion as a function of temperature were obtained within a single experiment. This is an important development because such measurements will be needed as control variables for the integrated SI thermochemical cycle. Further analysis of these large data sets is anticipated to yield additional information for use in the design of the next stage of experiments.

Pressure, temperature, and gas flow rate measurements were recorded every five seconds, and gas composition measurements were recorded every three minutes. Pressure was readily maintained at the desired preset level by using a pressure-relief valve. These valves are generally used as safety devices, but in our experiments, the valves were used as flow controllers. In future experiments it may be possible to identify a suitable commercial flow controller to maintain a set pressure, but none were available in the time frame of these tests. The pressure-relief valves did not vary the flow rate smoothly and at times introduced rapid variations in the flow rate. The result of these variations was scatter in the measured acid conversion fraction. This problem can be resolved by using a controller designed for smooth operations of a gas valve, and such a controller is planned for the next series of tests. The gas composition measurement problems with a gas chromatograph (GC) will also be resolved.

The data show the expected trend of increasing acid conversion fraction with increasing temperature, which is consistent with predictions. However, the measurements did not have the resolution needed to show the decrease in conversion fraction with increasing pressure. For acid vapor temperatures varying from 750 °C to 875 °C, the measured conversion fraction ranged from 0.4 to 0.45, respectively at six bars, and from 0.3 to 0.5, respectively at eleven bars. These values were bounded from above by the thermodynamic equilibrium limit for acid conversion. Real-time diagnostics were used for the first time in these types of experiments, which allows the conversion fraction to be available within seconds for process control, and chemical composition data to be available in minutes.

Much work on acid decomposition has been performed in the past using laboratory glassware. These materials, although high in corrosion resistance, are not generally practical for scale-up to a large production facility. Therefore, we are pursuing engineering solutions to the corrosion problem with innovative designs using industrial materials. In the current design, there was negligible pressure drop across the apparatus for the four and a half hours of acid processing. This was due to a combination of engineering designs that included (1) rapid heating to vaporize liquid acid before it contacted metallic walls, (2) a ceramic acid injection tube, (3) straight-through flow paths to minimize flow restrictions, and (4) rapid quenching of undecomposed acid vapors. Nonetheless, corrosion was observed as indicated by the green color of the collected liquid and green residue in the exhaust tube. We are in the process of disassembling the apparatus for detailed inspection of the

interior surfaces to determine the location of the corrosion. If corrosion occurred primarily in the condenser, then this problem may be eliminated with the new apparatus design that replaces the condenser with a direct contact heat exchanger (DCHX). The next phase of the acid decomposition experiments will not only employ the DCHX, but will also continue to improve materials and designs of other components to provide the technical basis for the integrated lab scale tests.

References

- Brecher, L. E., S. Spewock, and C. J. Warde, "The Westinghouse Sulfur Cycle for the Thermochemical Decomposition of Water," *International Journal of Hydrogen Energy*, Vol. **2**, pp. 7-15, 1977.
- Farbman, G. H., "The Conceptual Design of an Integrated Nuclear – Hydrogen Production Plant Using the Sulfur Cycle Water Decomposition System," Westinghouse Astronuclear Laboratory, Pittsburgh, PA, Report Number NASA-CR-134976, April 1976.
- General Atomics, "High-Pressure Catalytic Metal Reactor in a Simulated Solar Central Receiver," GA Technologies, GA-A18285, San Diego, California, February 1986.
- Hayduk, W. H. Asatani, and B. C. Y. Lu, "Solubility of Sulfur Dioxide in Aqueous Sulfuric Acid Solutions," *J. Chemical Engineering Data*, **33**, 506-509, 1988.
- HSC Chemistry 5.1, Outokumpu Research, Finland, October 2002.
- Lide, D. R. (ed.), CRC Handbook of Chemistry and Physics, 82nd edition, Boca Raton, Florida, 2001.
- Norman, J. H., G. E. Besenbruch, and D. R. O'Keefe, "Thermochemical Water-Splitting for Hydrogen Production," Final Report (January 1975 – December 1980), GRI-80/0105, March 1981.
- Parker, G. H., "Solar Thermal Hydrogen Production Process: Final Report December 1982," DOE/ET/20608-1, Westinghouse Electric Corporation, Advanced Energy Systems Division, Pittsburgh, Pennsylvania, 1982.
- Vargaftik, N. B. (ed.), Tables on the Thermophysical Properties of Liquids and Gases, 2nd edition, Hemisphere Publishing, Washington, 1975.
- Weast, R. C. (ed.), CRC Handbook of Chemistry and Physics, 70th edition, Boca Raton, Florida, 1988.

Electronic Distribution:

A. David Henderson
United States Department of Energy
Nuclear Hydrogen Research
Office of Nuclear Energy, Science and Technology
Germantown, MD 20874-1290
David.henderson@nuclear.energy.gov

Amy Taylor
United States Department of Energy
Nuclear Hydrogen Research
Office of Nuclear Energy, Science and Technology
Germantown, MD 20874-1290
Amy.taylor@nuclear.energy.gov

Merrill Wilson
Ceramatec
2425 South 900 West
Salt Lake City, UT 84119
Wilson@ceramatec.com

Charles A. Lewinsohn
Ceramatec
2425 South 900 West
Salt Lake City, UT 84119
clewinsohn@ceramatec.com

Alan Del Paggio
Critical Catalyst Company
Houston, Texas 77060
Alan.DelPaggio@cricatalyst.com

Gottfried Besenbruch
General Atomics
PO BOX 85608
San Diego, CA 92186-5608
besenb@gat.com

Lloyd. C. Brown
General Atomics
PO BOX 85608
San Diego, CA 92186-5608
Lloyd.Brown@gat.com

Benjamin Russ
General Atomics
PO BOX 85608
San Diego, CA 92186-5608
ben.russ@gat.com

Robert Buckingham
General Atomics
PO BOX 85608
San Diego, CA 92186-5608
buckingham@fusion.gat.com

Daniel M. Ginosar
Idaho National Laboratory
PO Box 1625
Idaho Falls, ID 83415-2208
daniel.ginosar@inl.gov

Thomas M. Lillo
Idaho National Laboratory
PO Box 1625
Idaho Falls, ID 83415-2218
tml@inel.gov

John Kolts
Idaho National Laboratory
PO Box 1625
Idaho Falls, ID 83415
koltjh@inel.gov

Maximilian B. Gorenssek
Savannah River National Laboratory
Building 773-42A
Aiken SC 29808
Maximilian.gorenssek@srs.gov

Jean-Marc Borgard
Commissariat a l'Energie Atomique
France
borgard@CARNAC.CEA.FR

Philippe Carles
Commissariat a l'Energie Atomique
France
Philippe.carles@cea.fr

MS0703	R. B. Diver, 6218
MS0734	A. Ambrosini, 6245
MS0734	T. M. Nenoff, 6245
MS0748	S. B. Rodriguez, 6863
MS0748	G. E. Rochau, 6863
MS0771	D. L. Berry, 6800
MS0771	J. E. Kelly, 6870
MS0888	D. G. Enos, 1823
MS0895	K. M. Alam, 8332
MS0895	D. A. Rivera, 8332
MS1141	E. J. Parma, 6872
MS3611	J. C. Andazola, 6872
MS3611	F. Gelbard, 6872
MS3611	G. E. Naranjo, 6872
MS3611	A. Reay, 6872
MS3611	P. S. Pickard, 6872
MS3611	C. E. Velasquez, 6872

Printed distribution

1	MS0945	Central Technical Files, 8945-1
2	MS0899	Technical Library, 4536



Sandia National Laboratories